Journal of Inorganic Biochemistry 234 (2022) 111871

Contents lists available at ScienceDirect

Journal of Inorganic Biochemistry

journal homepage: www.elsevier.com/locate/jinorgbio

Review Article

NMR of paramagnetic metalloproteins in solution: Ubi venire, quo vadis?

Inês B. Trindade [a], Anaísa Coelho [a], Francesca Cantini [b,c], Mario Piccioli [b,c,*], Ricardo O. Louro [a,**]

[a] Instituto de Tecnologia Química e Biológica António Xavier (ITQB-NOVA), Universidade Nova de Lisboa, Av. da República (EAN), 2780-157 Oeiras, Portugal
[b] Department of Chemistry, Magnetic Resonance Center (CERM), University of Florence, Via L. Sacconi 6, 50019 Sesto Fiorentino, Italy
[c] Consorzio Interuniversitario Risonanze Magnetiche MetalloProteine (CIRMMP), Via L. Sacconi 6, 50019 Sesto Fiorentino, Italy

ARTICLE INFO

Keywords:
NMR spectroscopy
Paramagnetic
Metalloproteins
Structural biology
Electronic structure
Metal homeostasis and trafficking

ABSTRACT

Metalloproteins represent a substantial fraction of the proteome where they have an outsized contribution to enzymology. This stems from the reactivity of transition metals found in the active sites of numerous classes of enzymes that undergo redox and/or spin-state transitions. Notwithstanding, NMR structures of metalloproteins deposited in the PDB are under-represented and NMR studies exploring paramagnetic states are a minute fraction of the overall database content. This state of affairs contrasts with the early recognition that paramagnetic proteins offer unique opportunities for structure-function studies which are not available for diamagnetic proteins. Recent development of novel pulse sequences that minimize quenching of signal intensity that arises from the presence of a paramagnetic center in metalloproteins is extending even further the range of systems which can be studied by solution-state NMR. In this manuscript we review solution-state NMR applications to paramagnetic proteins, highlighting the developments in both methodologies and data interpretation, laying bare the vast range of opportunities for paramagnetic NMR to contribute to the understanding of structure and function of metalloenzymes and biomimetic metallocatalysts.

1. Introduction

Metalloproteins play a central role in biology as can be appreciated by the fact that between 30 and 45% of all genome-encoded predicted proteins bind metals as cofactors that are essential to maintain the structure and/or the biological function [1,2]. These are often transition metals having open-shell electronic configurations which under physiological conditions leads to the presence of states containing unpaired electrons that can be probed to inform on the structure and reactivity of the cofactor and its protein [3–5]. Cofactors with open-shell electronic configuration are often associated with catalytic activity, therefore the unpaired electrons enlighten the regions of the proteins that are most interesting to understand their biological function.

NMR spectroscopy can explore the structure, dynamics and function of (metallo)proteins at atomic resolution [6]. The first spectrum of a metalloprotein in paramagnetic state was collected for ferricytochrome *c* in 1965, and soon it was extended to other proteins [7,8]. In this review, we will focus on the application of paramagnetic NMR to native metalloproteins in solution, particularly, on the characterization of the structure and electronic properties of their metallocofactors. The use of extrinsic paramagnetic tags to characterize proteins in general, and the use of solid-state NMR methods for the characterization of metalloproteins have been reviewed elsewhere and will not be covered here [9,10].

2. Cursory overview of paramagnetic NMR concepts

Like the NMR-active nuclei, electrons behave as magnetic dipoles when placed in a magnetic field. Consequently, the interaction between the unpaired electron and a nucleus can be mediated by chemical bonds (contact mechanism) or through space (dipolar mechanism). The distinguishing effect of the presence of unpaired electrons in a molecule derives from the fact that the magnetic moment of electrons is almost three orders of magnitude larger than that of protons. Therefore, the unpaired electron modifies the local magnetic field in its vicinity and causes pronounced effects in NMR spectra. The most visible are: unusual

* Corresponding author at: Department of Chemistry, Magnetic Resonance Center (CERM), University of Florence, Via L. Sacconi 6, 50019 Sesto Fiorentino, Italy.
** Corresponding author at: Instituto de Tecnologia Química e Biológica António Xavier (ITQB-NOVA), Universidade Nova de Lisboa, Av. da República (EAN), 2780-157 Oeiras, Portugal.
E-mail addresses: piccioli@cerm.unifi.it (M. Piccioli), louro@itqb.unl.pt (R.O. Louro).

https://doi.org/10.1016/j.jinorgbio.2022.111871
Received 26 January 2022; Received in revised form 16 May 2022; Accepted 19 May 2022
Available online 23 May 2022

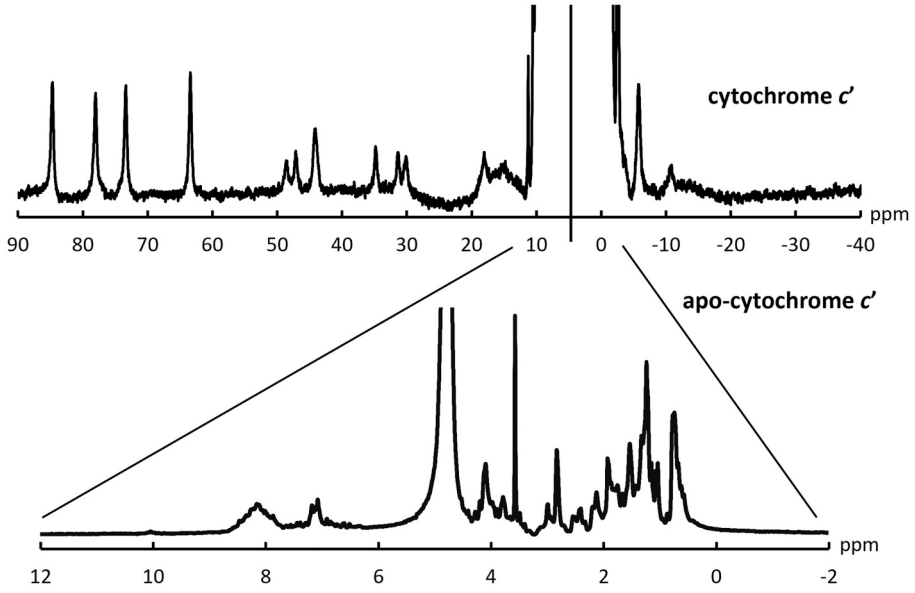

Fig. 1. ^{1}H NMR spectra, recorded at 500 MHz, of apo and holo-cytochrome c' from *Rhodobacter capsulatus*.

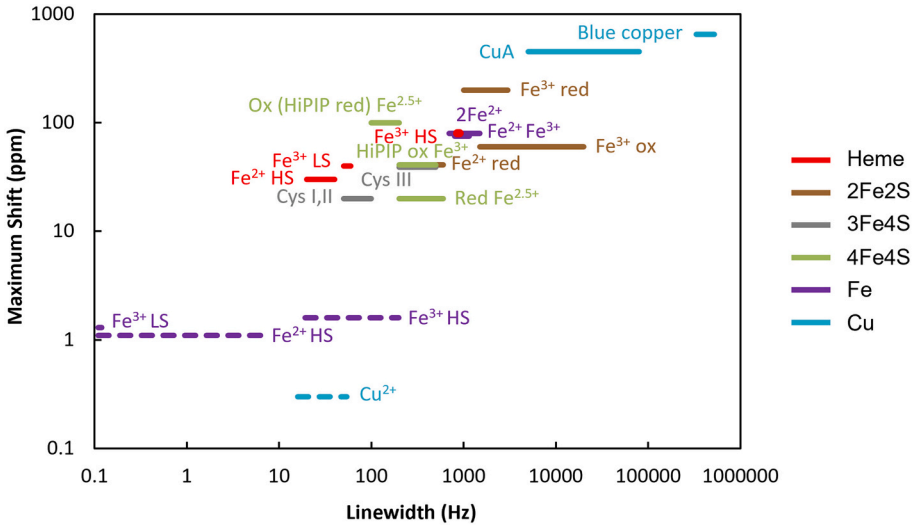

Fig. 2. Maximum chemical shift and typical linewidths ranges observed in metalloproteins for βCH_2 protons of cysteines coordinating iron-sulfur (FeS) clusters, βCH_2 protons of cysteines coordinating copper (Cu) sites, for exchangeable NH protons of histidines coordinating oxo-bridged clusters, and for heme methyls. Dashed lines correspond to pseudocontact shifts and linewidths for protons at 10 Å from the metal.

chemical shifts and temperature dependence of NMR signals affected by the unpaired electrons, and line broadening and enhanced nuclear relaxation rates (Fig. 1).

Electronic correlation times of metal centers span more than five orders of magnitude in the range from 10^{-13} to 10^{-8} s (Fig. 2) [11]. Therefore, nuclear relaxation properties of metal centers are diverse, and often require specialized strategies for spectral observation in each case [12].

2.1. *Effect of hyperfine coupling on NMR spectra: hyperfine shift*

The hyperfine interaction affects NMR chemical shifts and signal linewidths to different extents, which becomes a double-edged sword. On the one hand, paramagnetism can make the NMR investigation almost intractable, because signals can be broadened beyond detection or overwhelmed by sharp, diamagnetic signals. On the other hand, unique structural information can be obtained using tailored experimental approaches and by studying nuclei of low magnetogyric ratio such as ^{13}C and ^{15}N. (Fig. 3) [13,14]. Typically, the first step is the observation of NMR signals that are affected by the interaction with the paramagnetic center. The established strategy for their observation has two components: i) the acquisition of ^{1}H NMR spectra over large spectral windows using fast repetition rates for the suppression of slow relaxing protein signals and solvent; ii) the collection of a large number of scans for achieving sufficient S/N for very broad signals. WEFT (Water Eliminated Fourier Transform) and SUPERWEFT pulse sequences, more recently revised to include gradients, broadband pre-saturation and poly-chromatic pulses, are the most commonly used sequences for ^{1}H NMR data collection, allowing both solvent suppression and the observation of broad paramagnetic signals [15–17].

The properties of the orbitals associated with the unpaired electron (s) have an impact on the shift of the nuclei being observed. When unpaired electrons are in orbitals of overall spherical symmetry, the energy of the dipolar interaction between electrons and nuclei is averaged to

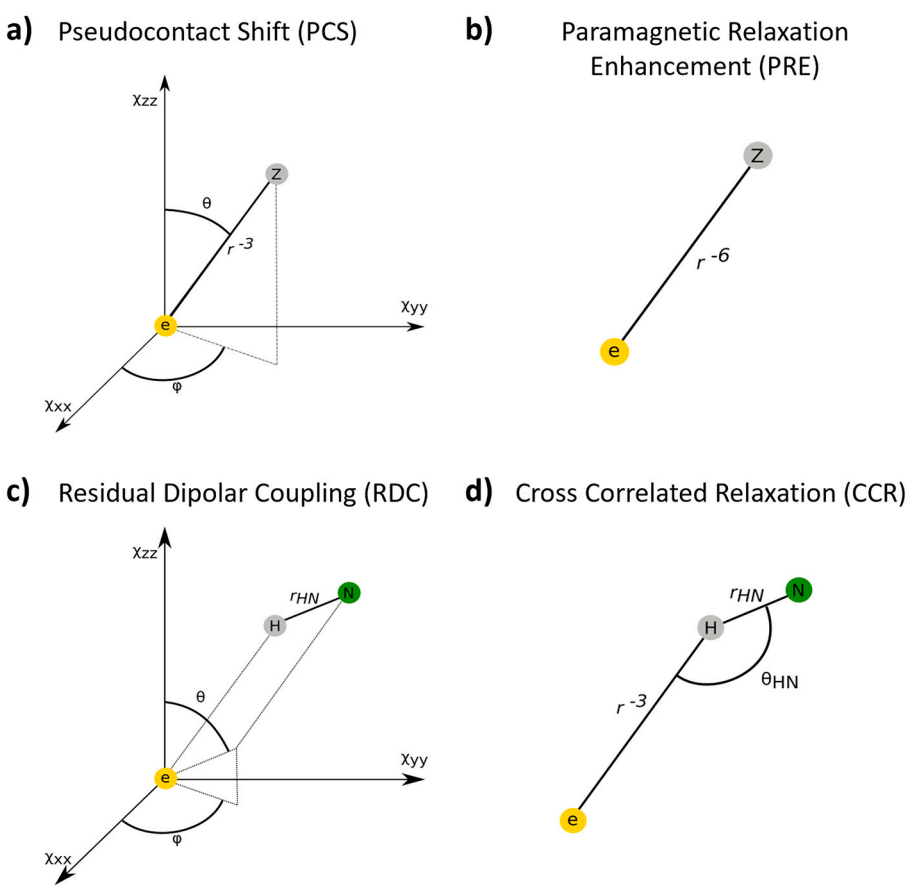

Fig. 3. Distance and geometric information that can be extracted from paramagnetic effects, caused by an unpaired electron considering the point dipole approximation (e) affecting any NMR active nuclei (Z), ^{1}H (H) or ^{15}N (N). (a) The Pseudocontact Shift (PCS) is dependent on the inverse third power of the distance between the nucleus and the paramagnetic center and upon the angular parameters θ and φ, relating the position of the nucleus under observation with the magnetic properties of the paramagnetic center. (b) Paramagnetic relaxation enhancements (PRE) depend upon the inverse sixth power of the distance between the electron and nuclear spin. (c) Paramagnetic residual dipolar couplings (RDC) between a ^{1}H and a ^{15}N spin depend on the angle between the bond connecting the coupled nuclei and the orientation of the magnetic axes that characterize the magnetic susceptibility tensor associated with the unpaired electron(s) (according to the angles θ and φ) and on the internuclear distance r_{HN}. (d) Cross correlation (CCR) between ^{1}H—^{15}N dipole-dipole relaxation and Curie relaxation for backbone amide H—N results in a measurable effect on the ^{1}H spin, which depends upon the inverse third power of the distance to the proton and on the angle, φ between the H—N vector and vector connecting the H and the unpaired electron.

zero by the isotropic molecular tumbling. In these conditions the chemical shift of the nuclei is not affected by dipolar interaction with the unpaired electron. If the unpaired electron can delocalize onto the nucleus being observed, its effect is propagated through the orbitals linking the paramagnetic center with the nucleus being observed. This is a scalar coupling, the value is independent of the molecular orientation in the magnetic field, and it is given by the hyperfine coupling constant [18,19]. The NMR signal of the nucleus will display Fermi contact shift that depends on metal ion, bond strength, electron delocalization mechanisms, number of bonds separating the nuclear spin from the metal, geometry of the paramagnetic center and dihedral angles of metal binding residues. When the unpaired electron(s) are found in orbitals of non-spherical symmetry, the energy of the dipolar interaction between the electron(s) and the nuclei does not average to zero by isotropic molecular tumbling. This gives rise to the pseudocontact shift (PCS) (Fig. 3A). It is dependent on the inverse third power of the distance between the nucleus and the paramagnetic center, on angular parameters relating the nucleus under observation with the magnetic properties of the paramagnetic center, and on the anisotropy and orientation of the magnetic susceptibility tensor (Fig. 3B) [20–23]. The hyperfine shift results from the sum of contact- and pseudocontact- shift terms: the interplay of the two contributions depends not only on the paramagnetic center, but also on the type of nucleus investigated and on its position within the protein frame [24].

2.2. Effect of hyperfine coupling on nuclear relaxation

Longitudinal relaxation (R_1) relates with the time necessary for the nuclear magnetization to return to equilibrium after excitation and is stimulated by fluctuations at frequencies near to the Larmor frequency. Faster relaxation means that Nuclear Overhauser Enhacement (NOE) intensities are quenched and shorter repetition times can be used in experiments. Transverse relaxation (R_2) is stimulated by fluctuations of frequency near to the Larmor frequency and lower. R_2 relates with linewidth of NMR signals, therefore faster relaxation leads to broader signals making their detection challenging.

The unpaired electron(s) enhance the relaxation of nuclear spins by three mechanisms, which are additive to “diamagnetic” nuclear relaxation: contact, dipolar and Curie spin relaxation. The extent and the relative contribution of each of these mechanisms to R_1 and R_2 is modulated by three phenomena that may affect the correlation time: i) electron relaxation; ii) molecular tumbling in solution and iii) chemical or conformational exchange [22].

For nuclei belonging to atoms of residues directly bound to the metal ion, contact relaxation is often the dominating mechanism. In contact relaxation, the correlation time is determined by the electron relaxation and by chemical exchange, when present. Therefore, R_1 and R_2 measurements provide a wealth of information on the extent of the interaction between the nuclei and the paramagnetic center and on the time dependence of this interaction. For nuclei belonging to atoms of residues not directly bound to the metal ion, the paramagnetic relaxation is dominated by the dipolar contribution. In this case, the relaxation rate becomes progressively slower with distance according to the inverse sixth power of the metal-nucleus separation since contact relaxation does not occur in these nuclei (Fig. 3B) [23]. Deviations from the r_{MX}^{-6} relationship occur when the unpaired electron spin density cannot be considered as fully localized on the metal ion. In the search for structural constraints, this is referred as the Paramagnetic Relaxation Enhancement (PRE) (Fig. 3B).

When placed in a magnetic field, electrons also display a preference for orienting in alignment with the field. This gives rise to an electronic magnetic moment called the Curie spin [25]. The interaction between the nuclear spin and the Curie spin is modulated by molecular tumbling and originates Curie spin nuclear relaxation. In macromolecules, the

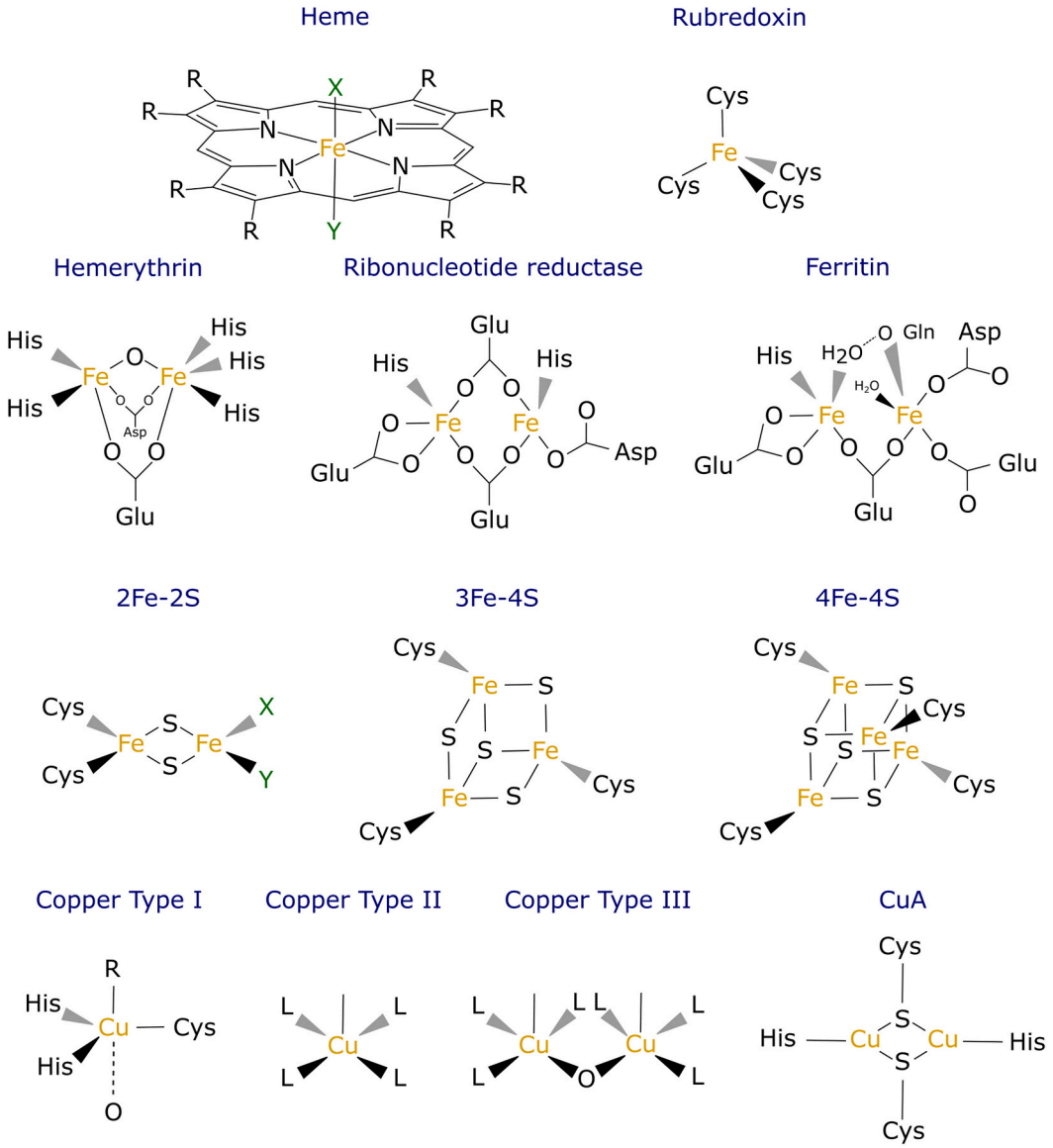

Fig. 4. Representation of the most common paramagnetic centers of proteins studied by NMR. In heme, X and Y represent a wide diversity of ligands where histidine and methionine are the most prevalent; in 2Fe—2S clusters, X and Y represent either cysteine and histidine (in case of mitoNEET) or two histidines (in case of Rieske proteins); in Copper Type I, R usually is methionine.

slow tumbling in solution creates a spectral density function dominated by frequencies that are lower than the resonance frequency set by the spectrometer. As a consequence, this relaxation mechanism is often dominant in R_2 but not R_1. Curie relaxation, like dipolar relaxation, depends upon the inverse sixth power of the metal-nucleus distance. It is given by the magnitude of the thermal average of the electron magnetic moments, which increases with the square of the static magnetic field of the spectrometer [25]. Therefore, the contribution of the Curie relaxation increases dramatically with the magnetic field and becomes important when the electronic relaxation is much faster (2–3 orders of magnitude) than the rotational tumbling of the molecule. Thus, as the molecular motion slows down, for instance, due to higher mass, higher viscosity of the medium or lower temperature, the contribution of Curie relaxation towards the total nuclear spin relaxation increases. For macromolecules at high magnetic fields, Curie relaxation can become dominant in R_2 and can lead to broadening of signals beyond detection [26]. This has been observed, for example, in the case of Co(II) substituted enzymes where, due to the high $S = 3/2$ electron spin and to the large rotational correlation time, several signals disappear from the ^{1}H NMR spectrum at increasing the magnetic field [27].

Dipolar and Curie relaxation are also proportional to the square of the gyromagnetic ratio of the nucleus under observation. Therefore, the effect of relaxation is more pronounced in protons and less intense in nuclei of lower gyromagnetic ratio such as ^{13}C ^{15}N. For this reason, ^{13}C or ^{15}N detected experiments have gained importance for the characterization of paramagnetic proteins and stimulated the development of detection probes designed for this purpose [28–30].

Additional contributions to relaxation come from the fact that relaxation mechanisms modulated by the same correlation time may interact with one another and originate cross correlating phenomena (CCR, Fig. 3D). This is the case of dipolar relaxation between coupled nuclei and Curie spin, which as mentioned above is field dependent. This leads to different line broadening of the various components of NMR multiplets [31]. The effect depends on the angle between the vector connecting the paramagnetic center with the investigated nucleus and the vector connecting the coupled nuclei, on the inverse third power of the distance and on the magnetic field strength (Fig. 3D).

2.3. Paramagnetically induced residual dipolar couplings

When the unpaired electron is found in orbitals that do not display spherical symmetry (anisotropic), there is an energetic preference for having the direction of strongest magnetic susceptibility aligned with the external magnetic field. At high fields, this preference makes a residual but noticeable effect on the motion of paramagnetic molecules, which is no longer isotropic. As a consequence, residual dipolar couplings (RDCs) (Fig. 3C) between nuclei typically become sufficiently large to be measured above 500 MHz, in the absence of orienting media [32,33]. These provide information on the angle between the bond connecting the coupled nuclei and the orientation of the principal directions of the molecular susceptibility tensor [23]. This effect is unique relative to those reported above because it does not depend on distance or number of bonds to the paramagnetic center [34].

2.4. Exploitation of low gyromagnetic ratio nuclei

Unlike the hyperfine shift, paramagnetic relaxation is dependent on γ^2: when passing from ^{1}H to ^{13}C detected experiments, the paramagnetic contribution to relaxation will be scaled during acquisition according to a factor $(\gamma_H/\gamma_C)^2$. The ^{13}C direct detection has been applied in copper proteins and in Ln(III)-substituted Calcium binding proteins, significantly reduced the blind sphere due to paramagnetism around the metal ion [35–37]. When ^{1}H spins are broadened beyond detection, ^{2}H spin may remain observable and helpful to characterize the first coordination sphere of metal ions with slow, unfavorable, electron relaxation times such as high spin Fe^{3+} of rubredoxins [38]. Together with ^{13}C, the direct detection of ^{15}N may elucidate the delocalization of unpaired spin density occurring not only trough coordination bonds but also via H-bonds [39,40]. Indeed, the direct detection of low gyromagnetic ration nuclei has been extremely useful for an increasing number of systems such as intrinsically disordered and proline-rich proteins, and molecules affected by chemical exchange [28,41]. Among the very many ^{13}C detected experiments developed, the ^{13}C—^{13}C COSY (COrrelation SpectroscopY) and the CACO (C^{α}-C′ correlation) were specifically tailored to paramagnetic systems [29,42,43].

2.5. Which metals are addressed in this review

All of the distance and geometric information that derives from the presence of a paramagnetic center has been crucial for obtaining the solution structure of metalloproteins and has allowed the investigation of the electronic structure of the active site of metalloproteins by NMR spectroscopy. This complements the experiments performed at cryogenic temperatures using other spectroscopies, such as Mössbauer and EPR but it also explores excited electronic states when they are thermally populated at physiological temperatures. This can be achieved by measuring the temperature dependence of the signals and fitting the data using the VanVleck formalism [11,44,45]. The analysis of the temperature dependence of NMR signals has a pivotal role for the study of magnetically coupled systems as well as in the cases of spin admixture and chemical exchange. This work on the electronic structure and geometry of paramagnetic metallic cofactors in proteins evolved from well-established investigation in inorganic chemistry [46–48]. Due to a combination of biological interest and more favorable electronic properties, hemes, iron-sulfur clusters and copper centers have attracted more attention than other systems (Fig. 4). A search in the Web of Science database for protein NMR plus copper, heme or iron gives an output that is at least one order of magnitude larger than when the second search term is replaced by vanadium, manganese, cobalt, nickel, or molybdenum. This review focuses on the analysis of paramagnetic iron and copper proteins.

3. Brief historical context of the origin of application of paramagnetic NMR to biological molecules

Heme proteins play many key roles in biology and their study was central to the development of biochemistry [49]. Due to their favorable spectroscopic features, they became early targets of NMR studies and the first spectrum of a metalloprotein was that of cytochrome *c*. Kowalsky observed signals downfield of the main protein envelope that were, for the first time, attributed not only to the “ring current model” of the porphyrin but also attributed to the magnetic properties of the iron [50]. Kowalsky further explored these observations and reported that the unusual resonances were the result of electron delocalization with consequent hyperfine contact interaction between the electron and certain protons of the heme or of the protein [7]. Subsequent work immediately revealed the power of paramagnetic NMR to characterize the structure of the paramagnetic cofactor with greater detail than that available by X-ray crystallography at the time [51]. In the same period the first measurements by NMR of magnetic susceptibility of ferredoxin from *Costridium pasteurianum* were taking place and the importance of interpreting resonances outside the crowded diamagnetic region of proteins started to gain its relevance [52,53]. In 1968, the temperature dependence of resonances of cyanometmyoglobin showed the possibility of distinguishing between shifts arising from hyperfine interactions and other mechanisms [51,53]. In 1970 the first spectra of an iron-sulfur protein and the temperature dependence of low field resonances were reported, giving rise to the first proposed model of cysteine-iron bonding in the ferredoxin from *Clostridium pasteurianum* [54]. This type of spectroscopic studies in metalloproteins became popular in the following years, when the development of the WEFT and SUPERWEFT pulse sequences contributed to overcome the problems of dynamic range and allowed the utilization of water as solvent without compromising the observation of the considerably broadened contact-shifted proton signals [15,55]. This boosted the elucidation of the electronic structure of the different paramagnetic centers in metalloproteins [56–60].

Notwithstanding, the structure determination of paramagnetic proteins lingered languished for a few years because the fast nuclear R_1 and R_2 hampered the detection of dipolar and scalar connectivities and adequate force field energy minimization parameters were difficult to select. Selective 1D NOEs and two-dimensional experiments were fundamental to overcome the loss of information around the metal center. In 1994, after assigning the missing connectivities in the vicinity of the paramagnetic center, the first solution structure of a paramagnetic protein was published: the High Potential Iron Sulfur Protein (HiPIP) from *Ectothiorhodospira halophila* in its reduced $[Fe_4S_4]^{2+}$ form (PDB ID: 1PIH) [45–49]. In the same year, Pochapsky reported the structure of a 2Fe—2S ferredoxin. However, unlike the previous example, the missing connectivies in the vicinity of the 2Fe—2S cluster hampered the quality of the model (PDB ID: 1PUT) [61]. One year later, the first structure of a paramagnetic heme protein was reported. It was the cyanide adduct of a Met80Ala variant of *Saccharomyces cerevisiae* Iso-1-cytochrome *c* using the assignment of hyperfine-shifted signals and NOE constraints (PDB ID: 1FHB) [62,63]. For copper proteins, the detailed characterization of the metal binding site was often made by metal substitution [64]. Indeed, paramagnetic copper proteins were for a long time considered non-tractable by NMR spectroscopy because of extreme broadening of resonances around the Cu^{2+} center. It was the recognition of different electron relaxation properties of blue vs non-blue copper proteins that opened the route to paramagnetic NMR of blue copper proteins [35,65]. As a consequence, the first solution structure of a paramagnetic copper protein was reported only in 2001, an oxidized plastocyanin from the cyanobacterium *Synechocystis* PCC6803 (PDB ID: 1J5C) [66]. Today, 26 years after the first structure of the nearly 12,000 NMR protein structures deposited in the PDB, about 12% are metalloproteins and only about 1% are paramagnetic metalloproteins [67]. This highlights both the enduring perception of the challenges of studying these systems by NMR spectroscopy, and the vast untapped potential that this approach

Table 1
Number of entries in the protein data bank for different search categories.

Total proteins PDB	162,477
(metalloproteins)	81,723
Total proteins by NMR	13,526
(metalloproteins)	1560
Total paramagnetic proteins by NMR	115
(Co)	3
(Cu)	8
(Fe)	95
(Ni)	4
(Fe—Cu)	5

holds (Table 1).

4. In the beginning there was iron

Iron-proteins have been the most extensively studied metalloproteins; not only because of their biological significance but also because iron centers can be characterized by several, and often complementary spectroscopies. In biological systems, iron is typically found as Fe^{3+} and Fe^{2+}. With the exception of octahedral Fe(II) with strong field axial ligands such as histidines, methionines and lysines, all iron centers in proteins have paramagnetic states at physiological temperature. For iron-proteins, the extent of paramagnetic effects varies greatly depending on the iron center and oxidation state [24].

4.1. Heme proteins

In heme proteins, the chemical shift of the signals of the substituents at the periphery of the heme ring has a strong contribution from the contact shift that results from mixing of the iron d orbitals with the porphyrin π orbitals [68]. This leads to the delocalization of the unpaired electron onto the porphyrin, which is modulated by the orientation of the axial ligands. The resulting contact shift is defined by the position where the axial ligands are projected on the heme plane. It is also defined by their dynamics, for instance with inversion of the axial methionine diasterioisomers at frequencies similar to the Larmor frequency [69–73]. This applies for both low-spin and high-spin states and for a variety of axial ligands [64–66]. Therefore, based solely on the assignment of the substituents at the periphery of the heme, it is possible to define the orientation of its axial ligands, and thus characterize the geometry and dynamics of the active site of hemeproteins, or enzyme mimics containing hemes (Fig. 5) [62,69–71,74–79].

In both low- and high-spin heme proteins the temperature dependence of the shifts of some heme methyls shows significant deviations from the 1/T expected from the Curie law. This reveals the presence of thermal population of the first excited electronic state in addition to the ground state and does not entail a change in the heme geometry or the position of the axial ligands with temperature [70,81,82].

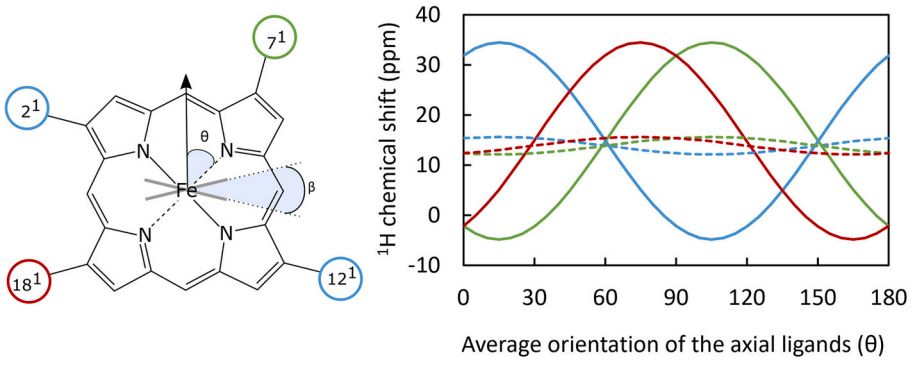

Fig. 5. ^{1}H chemical shift of the methyls at the periphery of the heme calculated for the case of low-spin hemes at 298 K, with two axial histidines with a relative angle β of their aromatic planes of 5 (continuous line) and 85 degrees (dashed line) [80]. Corrections due to the asymmetric placement of the vinyls in hemes *b*, or thioether bonds to cysteines in the case of hemes *c*, in the periphery of the heme were proposed but are not included in this representation. These corrections lift the degeneracy of the shifts of methyl 2^1 and methyl 12^1, with methyl 12^1 having a downfield shift larger than methyl 2^1 [61]. Matching the peak positions in the spectra with the lines in the figure allows for a simple determination of the orientation of the axial ligands. The right panel shows the diagram of the geometry of the axial ligands where θ is the average orientation of the axial ligands.

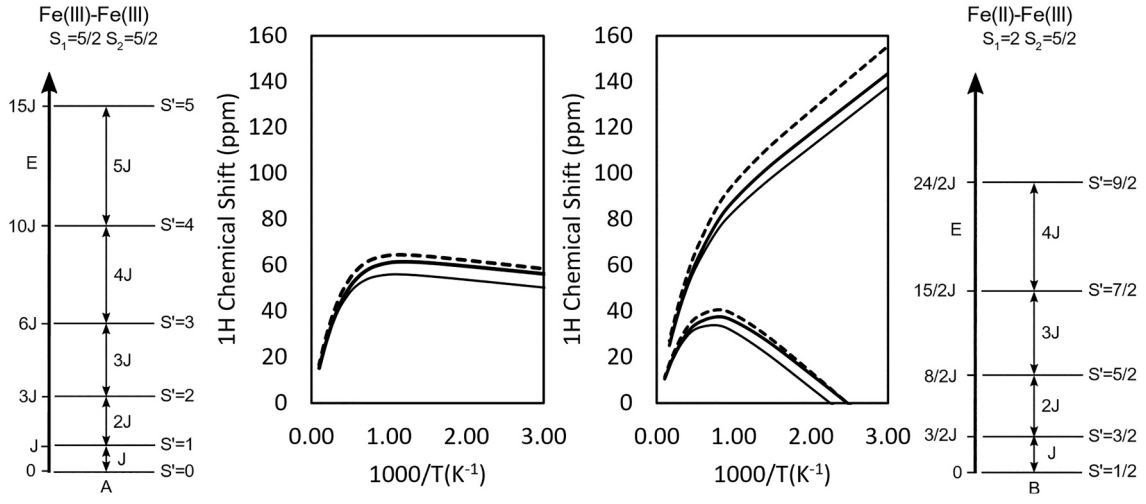

Fig. 6. Effect of magnetic coupling for the case of a 2Fe—2S cluster. The spin-state ladder for the oxidized and reduced states is shown on the left and right hand sides, with calculated temperature dependence of the paramagnetic shifts of signals of the ligands in the center. The thin and dashed lines report an increase of 10% of exchange coupling constant or of hyperfine electron-nuclear coupling, respectively, relative to the arbitrary reference values (J = 200 cm^{-1} and A = 1.81 MHz) giving the thick line, to illustrate the effect of these two parameters.

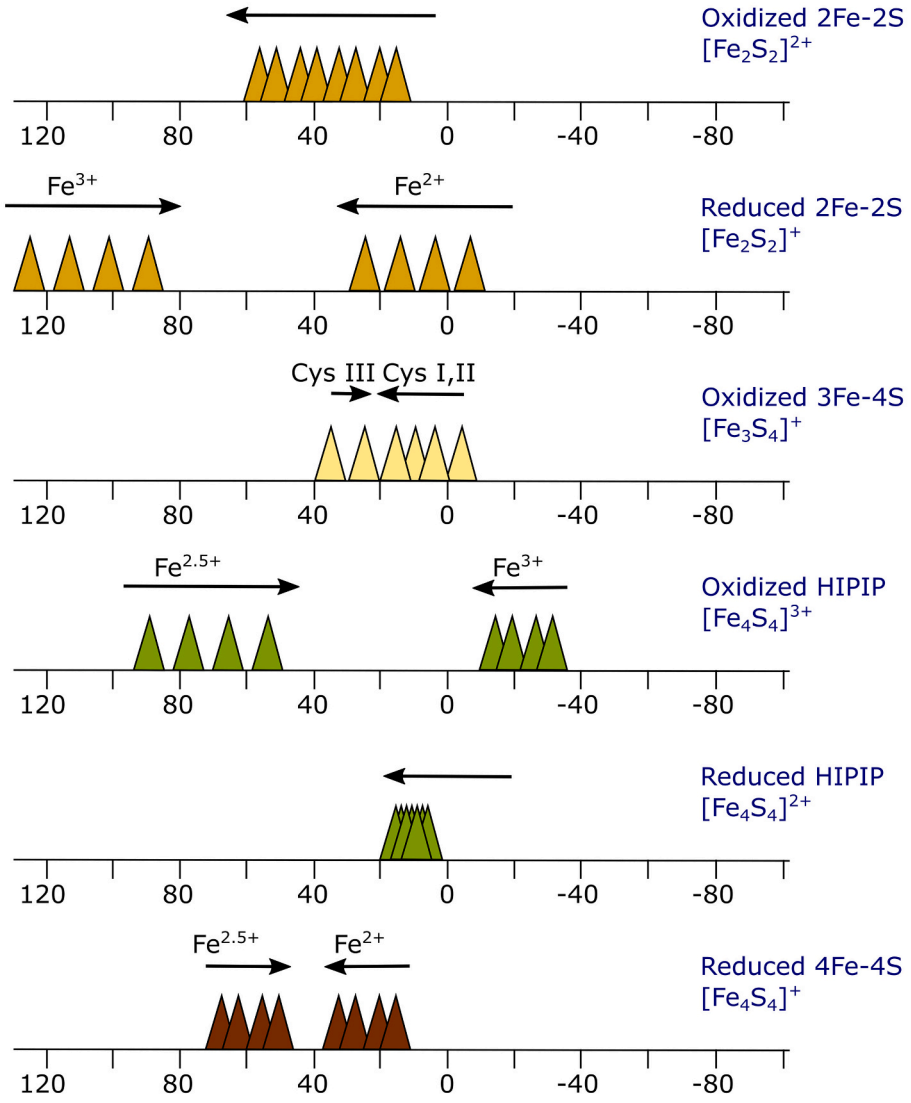

Fig. 7. Typical position and temperature dependence of the signals of coordinating cysteines in various FeS clusters in distinct redox states. Arrows indicate direction of change in chemical shift of the signals upon temperature increase.

4.2. Iron-sulfur proteins. The effect of magnetic coupling on the NMR parameters

Iron-sulfur clusters are likely among the oldest metallic cofactors in biology [83,84]. Except for rubredoxins, that contain a single iron, all metal centers of iron-sulfur proteins are polymetallic, where each of the iron atoms is coordinated in approximate tetrahedral geometry to inorganic sulfide ions of the cluster and to the polypeptide by cysteine side chains, in the vast majority of the cases, or by cysteines/histidine(s) or cysteines/serine coordination (Fig. 4) [85].

In 2Fe—2S clusters the two iron ions are linked by two bridging inorganic sulfide ions. In ferredoxins each iron is coordinated by two cysteines, whereas in mitoNEET-type and Rieske-type proteins one of the iron ions is coordinated by respectively, one or two histidines (Fig. 4). The iron ions are antiferromagnetically coupled. In the oxidized state this coupling between two, high-spin, Fe^{3+} ions leads to a $S = 0$ ground state even though a significant paramagnetism may occur at room temperature due to thermal population of excited paramagnetic states, as shown in Fig. 6 [86]. This gives rise to paramagnetically shifted signals which increase their shift with increasing temperature, the so-called anti-Curie behaviour (Fig. 7). This has been used in the study of iron-sulfur proteins containing 2Fe—2S and 4Fe—4S clusters, to identify the oxidation state of the cluster and its electronic structure. The two iron ions of the 2Fe—2S cluster are not equivalent due to differences in their primary (Rieske and mitoNEET proteins) or secondary (ferredoxins) coordination sphere and, upon reduction, the electron tends to be localized in one of them giving rise to a localized mixed valence cluster [44]. However, the electronic state of reduced 2Fe—2S clusters (Fig. 6) is also affected by the ability of 2Fe—2S clusters to exchange one electron between the two iron ions due to double exchange mechanism; the predominance of localized vs delocalized valence can be driven by subtle structural factors [87,88]. In Rieske-type ferredoxins the iron coordinated to the histidines is the one that is redox active [89]. The larger spin of the high-spin Fe^{3+} aligns with the magnetic field and the signals of the cysteines coordinating this iron display a large downfield shift and Curie type temperature dependence. By contrast, the smaller spin of the high-spin Fe^{2+} is anti-parallel to the field and the signals of its coordinating cysteines (histidines in Rieske type proteins) display anti-Curie temperature dependence (Fig. 7) [86]. This offers the unique opportunity to identify the redox active iron in the cluster. The fact that the temperature dependence of the signals does not follow a strict Curie dependence reveals the population of excited spin states at room temperature. The exchange coupling constant between the irons increases from ~100 cm^{-1} in the reduced state to ~200–300 cm^{-1} in the oxidized

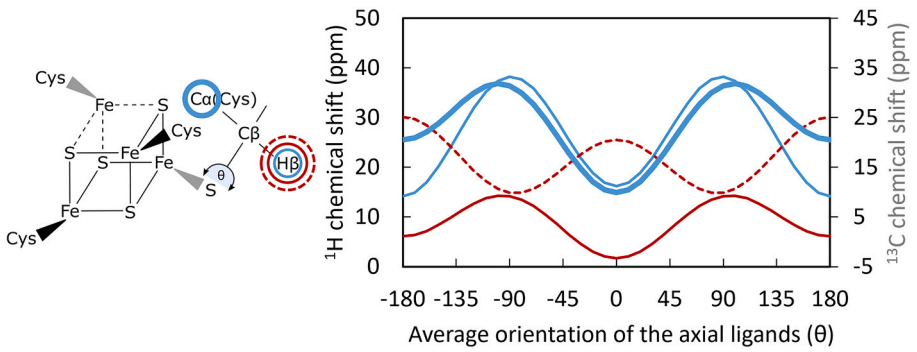

Fig. 8. Top: Geometric dependence of the hyperfine shift of β-CH protons and alpha carbons of cysteines attached to the cluster in oxidized ferredoxins and reduced HIPIPs [11]. Bottom: β-CH protons of cysteines coordinating strongly coupled irons and coordinating the more weakly coupled iron of oxidized $[Fe_3S_4]^+$ clusters [104]. Angles refer to the dihedral angle with the Fe-Sγ bond and matching the position of the peaks with the lines in the figure allows for an easy determination of the dihedral angles that are compatible with experimental data.

state for various proteins [44,45,90]. This shows that the magnitude of the exchange coupling constant is determined by the architecture Fe_2S_2 rhomb and not by the chemical nature or geometrical distortions that might be caused by the protein ligands that bind the cluster [44,91].

In the case of 3Fe—4S clusters, the third iron ion cannot be antiferromagnetically coupled to both of the other two iron ions, a phenomenon designated spin frustration [92,93]. In the oxidized $[Fe_3S_4]^+$ cluster the three Fe^{3+} ions are not equivalent, with one pair more strongly coupled together than with the remaining iron [94–96]. As a consequence, the β-CH protons of cysteines coordinating the more strongly coupled irons (conventionally designated I and II) display anti-Curie behaviour whereas those of the more weakly coupled iron (designated III) are found more downfield and display a Curie type temperature dependence (Fig. 7) [95,97]. When the cluster is in the reduced, $[Fe_3S_4]^0$ state, valence delocalization occurs [98]. This means that an electron is shared by a pair of iron ions that assume a formal fractionary charge value of +2.5. The reduced form of these clusters has signals too broad to be detected.

For proteins containing 4Fe—4S clusters, valence delocalization is also observed [99]. In the case of ferredoxins, the cluster oxidizes from $[Fe_4S_4]^+$ to $[Fe_4S_4]^{2+}$ at low potential with the iron ions displaying the formal $2Fe^{2.5+}$- $2Fe^{2+}$ and $4Fe^{2.5+}$, respectively. In the case of HIPIPs the reduced state $[Fe_4S_4]^{2+}$ again contains $4Fe^{2.5+}$and oxidizes to $[Fe_4S_4]^{3+}$ with $2Fe^{2.5+}$ and $2Fe^{3+}$ [100]. In oxidized ferredoxins and reduced HiPIPs, the four irons are equivalent and antiferromagnetically coupled. The overall situation is therefore similar to the case of $[Fe_2S_2]^{2+}$ ferredoxins where the electron spin has a ground state S = 0 and paramagnetically shifted signals occur due to thermal population of low lying excited paramagnetic states. However, shorter electronic correlation times are observed for $[Fe_4S_4]^{2+}$ clusters, making the paramagnetically shifted ^{1}H signals of cysteine βCH_2 much sharper than for $[Fe_2S_2]^{2+}$ clusters. For oxidized HIPIPs and reduced ferredoxins, the β-CH protons of the cysteines coordinating the mixed valence irons are found at low field and with a Curie type temperature dependence (Fig. 7). The β-CH protons of the cysteines coordinating Fe^{2+} in reduced ferredoxins and coordinating Fe^{3+} in oxidized HIPIPs are less shifted and display anti-Curie behaviour. In the case of oxidized HiPIPs, where magnetic coupling is expected to be slightly larger than in ferredoxins, the β-CH protons of the cysteines coordinating Fe^{3+} are also found at high fields (<0 ppm) [101–103].

Proteins containing iron-sulfur clusters were early targets of studies by NMR spectroscopy, providing insights on the structure of the clusters that were unresolved by X-ray at the time [54]. These early investigations revealed that contact shifts influence the spectral position of the signals of the cysteine beta protons and alpha carbons. For $[Fe_4S_4]^{2+}$ clusters, contact shifts provide information on the dihedral angle between Fe-S-Cβ-Hβ or Fe-S-Cβ-Cα. This influence is modulated according to contributions of unpaired spin density in Fe—S σ bonds and in pπ bonds of the sulfur, with the latter being the dominant term [104,105]. This provides an important geometrical constraint to define the structure of the protein in the vicinity of the cluster, which is often difficult by other NMR observables such as NOEs due to fast paramagnetic relaxation [106] (Fig. 8).

Often the redox activity of a polymetallic cluster is confined to a single iron atom. Assignment of the resonances of the ligands of the irons in the cluster, allows to pinpoint the relevant iron [44,45]. This is a crucial mechanistic information because the rates of electron transfer decay exponentially with distance [3,107]. Furthermore, electrostatic interactions between partners depend on the presence and location of charges. These interactions contribute to recognition and transient binding between redox partners, and also depend exponentially with distance [108,109]. Indeed, iron-sulfur clusters are also involved in other metabolic pathways not directly related to biological electron transfer [110–112]. This opens the possibility to use paramagnetic NMR for example to elucidate iron-sulfur cluster assembly mechanisms within the mitochondrial matrix and to obtain insights onto the catalytic mechanisms of (Radical S-Adenosyl-L-Methionine) R-SAM enzymes [113–116].

4.3. *Non-heme, non-sulfur iron proteins*

Proteins containing iron clusters devoid of coordinating sulfur atoms play key roles in biology. Well researched examples are ribonucleotide reductases (Fig. 4) that are key enzymes for RNA synthesis, hemerythrins (Fig. 4) that transport oxygen in some marine invertebrates, and ferritins (Fig. 4) that perform iron storage in all domains of life. In these proteins two iron atoms are held together by oxygen atoms, either as bridging ligand or provided by carboxylates of amino acid sidechains of aspartates or glutamates [117–120]. In ferritins the two irons bind asymmetrically to the ferroxidase site as ferrous iron ions held together by a single carboxylate bridge. Upon binding of oxygen the ferrous irons are converted into diferric oxo groups that are stored in the internal cavity of the protein [120]. In ribonucleotide reductases and hemerythrin, the two iron atoms are held together by two carboxylate bridges. In ribonucleotide reductase the iron ions are hexacoordinated, whereas in hemerythrins the two iron ions have different coordination with pentacoordinated (Fe_a) and hexacoordinated (Fe_b) iron sites. These differences appear to impact on the redox properties of the two classes of proteins. Ribonucleotide reductases undergo a two-electron transfer from $2Fe^{3+}$ to $2Fe^{2+}$ coupled to transfer of one proton, whereas in hemerythrins the so called 'semi-met' state with one Fe^{3+} and one Fe^{2+} is easily obtained. For hemerythrins the electronic structure of the di-iron cluster was investigated by multiple spectroscopic methods, including paramagnetic NMR [121]. The iron atoms are antiferromagnetically coupled and this coupling varies with oxidation state, being considerably diminished in the semi-met and in reduced deoxy states. A trapped mixed valence state can be observed for the semi-met protein with the maximum shift, linewidth and temperature dependence of separate histidine imidazole NH resonances allowing assignment of the redox state of the Fe_a and Fe_b [121]. This is reminiscent of the situation observed in reduced 2Fe—2S clusters.

5. Then there was copper

Copper gained prominence as a biologically relevant metal with the advent of an oxidizing atmosphere, and copper containing proteins play key roles in aerobic metabolism [122]. Indeed, multicopper oxidases are very fast and efficient catalysts of oxidation reactions. Copper in biological systems alternates between the Cu^{+}/Cu^{2+} states.

Cu^{+} is diamagnetic, whereas Cu^{2+} has one unpaired electron and thus is paramagnetic. Copper proteins can have mononuclear copper centers or multi-copper centers, and these are usually typified according to their EPR spectra. Paramagnetically shifted NMR signals have been assigned to ligands of different kinds of mono- and multi-nuclear copper clusters [123]. This assignment allows the investigation of the nature of the ligands and their binding mode to the metal [124]. It also allows the investigation of the reaction mechanisms of copper enzymes. Changes in coordination of the copper ions and the formation and breakage of bridges during the reaction mechanism change the electronic coupling between the metals. This has an impact on the temperature dependence of the paramagnetically shifted signals [125].

Mononuclear copper centers can be classified into type I or type II (Fig. 4). Type I, typically represented by blue copper proteins, display a distorted trigonal geometry where the metal ion is strongly bound to two histidines and one cysteine. Often, a fourth weakly bound ligand (usually a methionine) can be found. A fast electron relaxation ($\tau_s \approx 10^{-10}$ s) occurs in these types of centers, as a result of the relatively small energy separation between the ground and excited states. Consequently, NMR signals of copper bound residues are detectable. Type II, typical of non-blue copper proteins, display a tetragonal geometry, as commonly found in "normal" tetragonal Cu^{2+} complexes where the metal ion is bound to four ligands. Despite the apparent normality, type II copper proteins present unique properties [126]. As consequence of the lack of low-lying excited electronic states, electronic relaxation is inefficient causing long correlation time for electron-nucleus interaction [127]. In comparison to type I copper proteins, this leads to dramatic line broadening of NMR signals of copper bound residues. For type II proteins, ^{13}C and ^{15}N nuclei can be used for signal assignment because of the lower gyromagnetic ratio of these nuclei [128].

Multicopper centers display relatively sharp NMR lines due to a decreased paramagnetism or a shorter electron relaxation time, as a consequence of the magnetic coupling. These properties can be used to explore the electronic structure of these systems and their physiological consequences. For example, the CuA center of multicopper oxidases, which are essential enzymes in aerobic respiration, has two spin-coupled copper ions in formal $Cu^{1.5+}$ oxidation state, with a thermally accessible excited state at room temperature [129]. A substantial degree of unpaired spin density is found in the bridging cysteine ligands and the order of the molecular orbitals in the ground and first excited state are predicted to change depending on the Cu-S-Cu angle [130]. The Karplus-like equation provides a linkage between the electronic and molecular structure of the cluster: a sine squared dependence on the Hβ-Cβ-Sγ-Cu dihedral angle is expected for the ground state σ_{u^*} while a cosine squared dependence is expected for the π_u state [131]. The fact that neither a sine squared, nor a cosine squared correlation is found for the shifts of the cysteine beta protons with the dihedral angle Hβ-Cβ-Sγ-Sγ means that, at room temperature, NMR is monitoring a temperature average of two states. Therefore, a substantial fraction of the π_u electronic excited state exists at the physiological temperature and argues for its participation in the electron transfer mechanism [129,131]. In the case of tyrosinase at room temperature, the oxidized Cu^{2+}-Cu^{2+} type III cluster has a diamagnetic ground state as a consequence of the antiferromagnetically coupling of the copper ions but an excited triplet state is thermally accessible giving rise to paramagnetically shifted signals. The temperature dependence of these signals, as well as their relaxation rates, showed that binding of chloride increases the exchange coupling between the copper ions and enhances the electronic relaxation [124]. In the case of laccases, another important group of multicopper oxidases, the electronic structures of the resting, oxidized and native intermediate states, can be distinguished. They show different degrees of coupling between the type II and type III sites and have markedly different oxygen to water reduction kinetics [123,125]. The most reactive native intermediate has three Cu^{2+} ions with spin ½ antiferromagnetically coupled. This leads to spin-frustration in which one of the copper ions has the spin aligned with that of one of its partners. This situation is akin to that observed for 3Fe—4S clusters.

As observed for iron-sulfur clusters, the contact shifts of copper coordinating cysteine atoms have an angular dependence on the dihedral angle, which were used as constraints to obtain the first solution structure of a blue copper protein in the oxidized Cu^{2+} state [66,132]. The structure of the mononuclear copper cluster of plastocyanin was determined from paramagnetic NMR restraints by dropping the point dipole approximation and correcting for the distribution of spin density of the unpaired electron onto the ligand atoms [133]. However, some kinds of copper clusters, notably type II casts a veil of invisibility over the signals of nuclei in their vicinity. Exploration of these systems required the development of dedicated protocols for structure determination in these proteins [128,134]. Indeed, in the next section it will be briefly shown that, although the strategy for solution structure of paramagnetic protein is "general", each different metallocofactor requires a specific treatment.

These developments, interesting by themselves in the contexts of spectroscopy and coordination chemistry, furthermore, enabled the study of cellular copper trafficking and homeostasis both in vitro and in vivo enabling the identification of insights relevant for intervention in numerous diseases [135,136].

6. Solution structures of metalloproteins, a current state-of the-art

Paramagnetism-based NMR restraints became a topic well beyond the enclave of metalloproteins over the last years. Many laboratories have promoted the use of paramagnetism-based NMR restraints to study diamagnetic proteins: metal binding tags have been used as spin-labels and provide restraints to complement the NMR information available [137–144]. However, tagged-proteins and metalloproteins are quite different. In the former cases, the paramagnetic binding tag is typically used to generate long range constraints, capable to provide structural information typically in a distance range of 10 to 40 Å. This can be accomplished either by measuring PCSs of highly anisotropic centers, typically Dy^{3+}, Tm^{3+} and other Ln^{3+} ions, or by measuring dipolar paramagnetic relaxation enhancement (PRE) [145,146]. The most useful spin-labels for PRE measurements are those with slow electronic relaxation rates and isotropic g-tensor, such as Cu(II) or Gd(III). The magnitude of PCS is proportional to r^{-3} (r being the metal-to-nucleus distance) and the magnitude of PREs is proportional to r^{-6} (Fig. 3). In both cases, long range interactions are very useful to identify intramolecular reorientations within proteins of large molecular weight or within multidomain proteins. PRE are also popular for elucidating structures of complexes, as they shed light into weak protein-protein/DNA/ions interactions [147–154]. In metalloproteins the situation is completely different from the case of spin labels: the environment of the metal center(s) is the core region for the protein function. Therefore, the goal is to obtain structural information, detailed as much as possible, in the close proximity of the metal. In this frame, reducing the blind sphere, obtaining structural restraints around the paramagnetic center and including them into structure calculations is crucial. In addition to the most widely used PREs and PCS, different types of paramagnetism based restraints have been introduced into structure calculation programs [155–158]. RDCs arising from self-orientation due to the paramagnetic susceptibility tensor, provide dipole orientations with respect to the molecular susceptibility tensor which, in paramagnetic systems, is often driven by the paramagnetic component [159]. Also, cross correlation rates have been included into structure calculations [160,161].

Table 2
Structural and electronic information that can be extracted from paramagnetic NMR experiments on selected metalloproteins.

Heme proteins	Orientation of the axial ligands
	Spin state of the iron
FeS proteins	Geometry of the coordinating cysteines
	Energy separation between electronic states
	Redox state of individual irons in the cluster
FeO proteins	Energy separation between electronic states
	Redox state of individual irons in the cluster
Cu proteins	Geometry of the coordinating cysteines
	Energy separation between electronic states

A relevant aspect for structure calculation is how the metal center is treated within software packages for biomolecular structure determination such as Xplor-NIH or CYANA [162–166]. In the case of CYANA, the easiest approach to include one or more metal ions is to append a chain of linker residues to the amino acid sequence. At the end of the linker, an atom with a radius mimicking the target metal ion is added. The linker residues have pseudo-atoms with van der Waals radii set to zero. The atoms of the ligands can be linked to the metal ion through upper and lower distance limits. With this approach, which has been used for Cu^{2+} containing proteins, the metal ion is located within the protein frame by using PRE restraints. Typically, the latter are obtained using ^{1}H relaxation at larger metal to proton distances and, in a closer shell from the metal, using ^{13}C PRE restraints [128]. When more complex cofactors are needed, such as iron-sulfur clusters or heme moieties, the definition of their molecular topology, is required. The library file needs to contain a description of atom types and nomenclature, covalent connectivities and geometry of the cofactors. To facilitate this process, an algorithm named CYLIB was developed for converting small molecule ligands and non-standard amino acid residues of the PDB Chemical Component Dictionary into CYANA residue library entries [167]. The non-standard library is subsequently appended to the standard CYANA library file with a unique"residue" identifier (e.g. SF2; SF4…). Finally, as structure calculations in torsion angle space requires that all components of the system should be linked by covalent bonds in a single chain, the cofactor must be incorporated into the protein with the same procedure used for a single metal ion.

An alternative approach is to prepare a modified version of the residues that link the metal center and append the definition of these modified residues to the standard CYANA library file. In the case of iron-sulfur clusters the ligand cysteines were substituted by a cysteinyl residue in which the thiol hydrogen (Hγ) replaced by an iron atom (Feδ) at the proper distance and by adding to the latter, through another covalent bond, the sulfur atom (Sε) constituting the inorganic sulfide of the cluster. Bond lengths and angles used in this construction need to be defined. Additional covalent bonds are added as link statements between each iron atoms (Feδ) and the bonded sulfur atoms (Sγ and Sε) [168]. For *c*-type cytochromes, two strategies were devised. One of them involved the use of a heme topology connected by the $C3^1$ and $C8^1$ to the Sγ atom of the two cysteines of the CXXCH heme binding that were modified to cysteinyl residues [168]. In the other strategy the second cysteine of the CXXCH heme binding motif was modified to have the Sγ connected to the $C8^1$ atom of a heme that is flexible through torsion angles associated with the bonds between the pyrroles and the *meso* carbons. The first cysteine of the heme binding motif was modified to a cysteinyl residue and a bond defined to bind the Sγ to the $C3^1$ atom of the heme. Axial histidines were replaced by hystidynil residues with the Ne^2 linked to an iron pseudoatom that overlaps with the iron of the heme to establish the hexacoordinate geometry [169].

Finally, the output of a CYANA calculation, the conformers with lowest target function values, are usually subjected to restrained energy minimization and Molecular Dynamics calculations with AMBER (D.A. Case et al. University of California, San Francisco). The refinement calculation is performed in explicit water with suitable force field parameters to treat the metal centers. These parameters cannot be generalized, nor be easily automated, and hence should be obtained for each system separately [170–172].

7. Future perspectives

The previous sections showed the potential for paramagnetic NMR to contribute to the structural and functional characterization of metalloproteins and metalloenzymes, which is summarized in Table 2.

There are exciting perspectives on the theoretical, instrumentation, methodological and biological fronts for their future study by NMR. Their structure and interactions can nowadays be monitored in vivo or *in cell*, thus opening unique opportunities to address biological functions [173,174].

On the theoretical front, there is renewed interest in replacing the classical semi-empirical description of the paramagnetic effect developed over the last 70 years with first principles quantum chemical calculations [175–177]. Ab-initio calculations of paramagnetic shifts and susceptibility, contributed to design ad-hoc paramagnetic probes and to compute paramagnetism-based structural restraints [178–180]. Relaxation anisotropy, intermolecular interactions, cross correlation, charge delocalization, pose still open questions on the accuracy of paramagnetic relaxation as structural restraints [179,182–184]. Recent

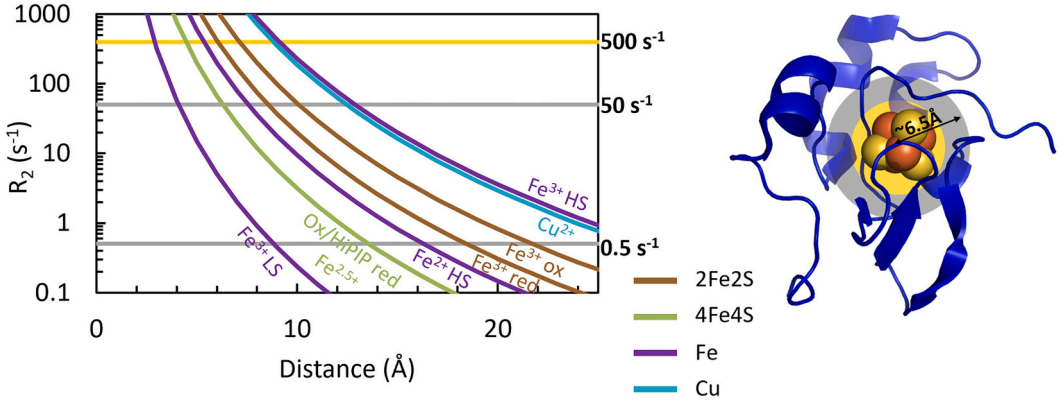

Fig. 9. Limits of detection of protons around different kinds of paramagnetic centers. The line at 50 s^{-1} represents the detection limit for (Heteronuclear Single Quantum Coherence) HSQC based experiments. The line at 500 s^{-1} represents the detection limit of novel R_2-weighted HSQC-AP (Anti-Phase) experiments [106]. R_2 calculated for a proton at various distances from the paramagnetic center in a protein of moderate size ($\tau_r = 1.5 \times 10–8$ s^{-1}) at 800 MHz. The line at 0.5 s^{-1} marks the limit of detection of the paramagnetic effect. The image on the right-hand side shows the impact of contracting the limit of detection on the characterization of paramagnetic metalloproteins.

developments in EPR spectroscopy open the possibility of guiding these efforts by probing experimentally the deviations from the point dipole approximation [185].

Also on the methodological front, ingenious developments of NMR pulse-programs are whittling away at the drawbacks of the paramagnetic effect on coherence transfer. For example, the time-scale of ^{1}H R_2 that can be measured has recently been increased from ~50 s^{-1} to 500 s^{-1} [106,186]. This significantly contracts the radius of the sphere around the paramagnetic center where signals cannot be observed, as shown in Fig. 9.

The effect is more pronounced the slower the electronic relaxation rate or the higher the spin-state with contractions of more than 4 Å for proteins containing high-spin Fe^{3+} or containing Cu^{2+}.

Last but not least, nature is a continuous source of surprises and opportunities. The recent realization that lanthanides may be the physiological metal cofactors of some proteins offers new targets which paramagnetic NMR is exquisitely suited to engage [187,188].

All of these can contribute to move paramagnetic protein NMR closer to the mainstream. Paramagnetic metalloproteins studied by NMR are woefully underrepresented in the PDB. A search on the Web of Science database for paramagnetic protein NMR reveals an annual publication output of approximately 100 papers vs approximately 2500 papers fulfilling the search criteria protein NMR. Given the undisputed relevance of metalloproteins and metalloenzymes for biological processes and for biotechnological applications, there is a vast untapped potential for application of NMR to the study of the structure and function of paramagnetic metalloproteins. Noticeably, this potential can be explored also on the cheap. Curie relaxation makes, for many cases, the study of paramagnetic metalloproteins less convenient at high field, alleviating the pressure to participate in the current race to install supra-GHz spectrometers to stay in the game. Additionally, field dependent effects such as cross correlations, molecular orientation and relaxation anisotropies promise to open new possibilities to exploit paramagnetic centers via NMR spectroscopy.

Declaration of Competing Interest

The authors declare that they have no known competing financial interests or personal relationships that could have appeared to influence the work reported in this paper.

Acknowledgements

The authors are grateful to Manuel Melo for making available algorithms for data mining from the PDB. The authors also thank Ana Silva and Nazua Costa for the ^{1}H NMR spectra of cytochrome c'. This work benefited from access to CERM/CIRMMP, the Instruct-ERIC Italy center, and CERMAX, ITQB-NOVA, Oeiras, Portugal with equipment funded by FCT, project AAC 01/SAICT/2016. Financial support was provided by European EC Horizon2020 TIMB3 (Project 810856) Instruct-ERIC (PID 4509). Financial support was also provided by Project MOSTMICRO-ITQB with refs UIDB/04612/2020 and UIDP/04612/2020. Fundação para a Ciência e a Tecnologia (FCT) Portugal is also acknowledged for funding through project PTDC/BIA-BQM/30176/2017, and through FCT PT-NMR PhD Program via PD/BD/135187/2017 and PD/BD/135153/2017 to IBT and AC, respectively.

References

[1] K.J. Waldron, J.C. Rutherford, D. Ford, N.J. Robinson, Metalloproteins and metal sensing, Nature 460 (2009) 823–830, https://doi.org/10.1038/nature08300.
[2] C. Andreini, I. Bertini, G. Cavallaro, G.L. Holliday, J.M. Thornton, Metal ions in biological catalysis: from enzyme databases to general principles, J. Biol. Inorg. Chem. 13 (2008) 1205–1218, https://doi.org/10.1007/s00775-008-0404-5.
[3] H.B. Gray, Chemical Bonds: An Introduction to Atomic and Molecular Structure, University Science Books, 1994, https://doi.org/10.7907/rt7h-8t44.
[4] I. Bertini, G. Parigi, C. Luchinat, E. Ravera, NMR of paramagnetic molecules, in: Applications to Metallobiomolecules and Models, 2nd ed, Elsevier, 2015, https://doi.org/10.1016/C2013-0-18690-4.
[5] W.R. Hagen, Biomolecular EPR Spectroscopy, CRC Press, 2008, https://doi.org/10.1201/9781420059588.
[6] P.J. Barrett, J. Chen, M.K. Cho, J.H. Kim, Z. Lu, S. Mathew, D. Peng, Y. Song, W. D. van Horn, T. Zhuang, F.D. Sonnichsen, C.R. Sanders, The quiet renaissance of protein nuclear magnetic resonance, Biochemistry 52 (2013) 1303–1320, https://doi.org/10.1021/bi4000436.
[7] A. Kowalsky, Nuclear magnetic resonance studies of cytochrome c. Possible electron delocalization, Biochim. Biophys. Actu. 4 (1965) 2382–2388, https://doi.org/10.1021/bi00887a018.
[8] W.D. Phillips, M. Poe, Contact shifts and magnetic susceptibilities in Iron-sulfur proteins as determined from NMR spectra, Methods Enzymol. 24 (1972) 304–317, https://doi.org/10.1016/0076-6879(72)24077-0.
[9] G. Otting, Protein NMR using paramagnetic ions, Annu. Rev. Biophys. 39 (2010) 387–405, https://doi.org/10.1146/annurev.biophys.093008.131321.
[10] J. Malanho Silva, L. Cerofolini, S. Giuntini, V. Calderone, C.F.G.C. Geraldes, A. L. Macedo, G. Parigi, M. Fragai, E. Ravera, C. Luchinat, Metal centers in biomolecular solid-state NMR, J. Struct. Biol. 206 (2019) 99–109, https://doi.org/10.1016/j.jsb.2018.11.013.
[11] I. Bertini, C. Luchinat, G. Parigi, Solution NMR of Paramagnetic Molecules: Applications to Metallobiomolecules and Models, Elsevier, 2001.
[12] I.B. Trindade, M. Invernici, F. Cantini, R.O. Louro, M. Piccioli, Sequence-specific assignments in NMR spectra of paramagnetic systems: a non-systematic approach, Inorg. Chim. Acta 514 (2021), https://doi.org/10.1016/j.ica.2020.119984.
[13] V. Ghini, S. Chevance, P. Turano, About the use of ^{13}C-^{13}C NOESY in bioinorganic chemistry, J. Inorg. Biochem. 192 (2019) 25–32, https://doi.org/10.1016/j.jinorgbio.2018.12.006.
[14] S. Ciofi-Baffoni, A. Gallo, R. Muzzioli, M. Piccioli, The IR-15N-HSQC-AP experiment: a new tool for NMR spectroscopy of paramagnetic molecules, J. Biomol. NMR 58 (2014) 123–128, https://doi.org/10.1007/s10858-013-9810-2.
[15] T. Inubushi, E.D. Becker, Efficient detection of paramagnetically shifted NMR resonances by optimizing the WEFT pulse sequence, J. Magn. Reson. 51 (1983) (1969) 128–133, https://doi.org/10.1016/0022-2364(83)90109-9.
[16] A. Bondon, C. Mouro, PASE (PAramagnetic signals enhancement): a new method for NMR study of paramagnetic proteins, J. Magn. Reson. 134 (1998) 154–157, https://doi.org/10.1006/jmre.1998.1523.
[17] G. Helms, J.D. Satterlee, Keeping PASE with WEFT: SHWEFT-PASE pulse sequences for 1H NMR spectra of highly paramagnetic molecules, Magn. Reson. Chem. 51 (2013) 222–229, https://doi.org/10.1002/mrc.3929.
[18] S.I. Weissman, Hyperfine splittings in polyatomic free radicals, J. Chem. Phys. (1954) 1378–1379, https://doi.org/10.1063/1.1740399.
[19] H.M. McConnell, D.B. Chesnut, Theory of isotropic hyperfine interactions in π-electron radicals, J. Chem. Phys. 28 (1958) 107–117, https://doi.org/10.1063/1.1744052.
[20] H.M. Mcconnell, R.E. Robertson, Isotropic nuclear resonance shifts, J. Chem. Phys. 29 (1958) 1361–1365, https://doi.org/10.1063/1.1744723.
[21] R.J. Kurland, B.R. Mcgarvey, Isotropic NMR shifts in transition metal complexes: the calculation of the Fermi contact and pseudocontact terms? J. Magn. Reson. 2 (1970) 286–301, https://doi.org/10.1016/0022-2364(70)90100-9.
[22] I. Bertini, P. Turano, A.J. Vila, Nuclear magnetic resonance of paramagnetic metalloproteins, Chem. Rev. (1993) 2833–2932, https://doi.org/10.1021/cr00024a009.
[23] M. Piccioli, Paramagnetic nmr spectroscopy is a tool to address reactivity, structure, and protein–protein interactions of metalloproteins: the case of iron–sulfur proteins, Magnetochemistry 6 (2020) 1–21, https://doi.org/10.3390/magnetochemistry6040046.
[24] M. Piccioli, P. Turano, Transient iron coordination sites in proteins: exploiting the dual nature of paramagnetic NMR, Coord. Chem. Rev. 284 (2015) 313–328, https://doi.org/10.1016/j.ccr.2014.05.007.
[25] M. Gueron, Nuclear relaxation in macromolecules by paramagnetic ions a novel mechanism, J. Magn. Reson. 19 (1975) 58–66, https://doi.org/10.1016/0022-2364(75)90029-3.
[26] A.J. Vega, D. Fiat, Nuclear relaxation processes of paramagnetic complexes the slow-motion case, Mol. Phys. 31 (1976) 347–355, https://doi.org/10.1080/00268977600100261.
[27] I. Bertini, B.-H. Jonsson, C. Luchinat, R. Pierattelli, A.J. Vila, Strategies of signal assignments in paramagnetic metalloproteins. An NMR investigation of the thiocyanate adduct of the cobalt(II)-substituted human carbonic anhydrase II, J. Magn. Reson. (1994) 230–239, https://doi.org/10.1006/jmrb.1994.1080.
[28] W. Bermel, I. Bertini, I.C. Felli, M. Piccioli, R. Pierattelli, 13C-detected protonless NMR spectroscopy of proteins in solution, Prog. Nucl. Magn. Reson. Spectrosc. 48 (2006) 25–45, https://doi.org/10.1016/j.pnmrs.2005.09.002.
[29] T.E. Machonkin, W.M. Westler, J.L. Markley, 13C{13C} 2D NMR: a novel strategy for the study of paramagnetic proteins with slow electronic relaxation rates, J. Am. Chem. Soc. 124 (2002) 3204–3205, https://doi.org/10.1021/ja017733j.
[30] K. Furuita, T. Sugiki, M. Takamuku, Y. Hattori, M. So, Y. Kawata, T. Ikegami, T. Fujiwara, C. Kojima, Sensitivity enhancement by sequential data acquisition for 13C-direct detection NMR, J. Magn. Reson. 322 (2021), https://doi.org/10.1016/j.jmr.2020.106878.
[31] A.A. Bothner-By, P.J. Domaille, C. Gayathri, Ultra-high field NMR spectroscopy: observation of proton-proton dipolar coupling paramagnetic Bis[tolyltris(pyrazolyl)borato]cobalt(II), J. Am. Chem. Soc. 103 (1981) 5602–5603, https://doi.org/10.1021/ja00408a069.

[32] J.R. Tolman, J.M. Flanagant, M.A. Kennedy, J.H. Prestegard, Nuclear magnetic dipole interactions in field-oriented proteins: information for structure determination in solution (myoglobin/NMR/paramagnetic proteins), Proc. Natl. Acad. Sci. 92 (1995) 9279–9283, https://doi.org/92/20/9279.

[33] N. Tjandra, A. Bax, Direct measurement of distances and angles in biomolecules by NMR in a dilute liquid crystalline medium, Science. 278 (1997) 1111–1114, https://doi.org/10.1126/science.278.5340.1111.

[34] I. Bertini, C. Luchinat, G. Parigi, R. Pierattelli, NMR spectroscopy of paramagnetic metalloproteins, ChemBioChem. 6 (2005) 1536–1549, https://doi.org/10.1002/cbic.200500124.

[35] U. Kolczak, J. Salgado, G. Siegal, M. Saraste, G.W. Canters, Paramagnetic NMR studies of blue and purple copper proteins, Biospectroscopy. 5 (1999) 19–31, https://doi.org/10.1002/(SICI)1520-6343(1999)5:5+<S19::AID-BSPY3>3.0.CO;2-H.

[36] F. Arnesano, L. Banci, I. Bertini, I.C. Felli, C. Luchinat, A.R. Thompsett, A strategy for the NMR characterization of type II copper(II) proteins: the case of the copper trafficking protein CopC from *Pseudomonas syringae*, J. Am. Chem. Soc. 125 (2003) 7200–7208, https://doi.org/10.1021/ja034112c.

[37] I. Bertini, Y.-M. Lee, C. Luchinat, M. Piccioli, L. Poggi, Locating the metal ion in calcium-binding proteins by using cerium(III) as a probe, ChemBioChem. 2 (2001) 550–558.

[38] W.D. Phillips, M. Poe, J.F. Weiher, C.C. Mcdonald, W. Lovenberg, R. Krishnamoorthi, J.L. Markley, A. Cusanovich, C.T. Przysieki, Detection and classification of hyperfine-shifted 1H, 2H, and 15N resonances from the four cysteines that ligate Iron in oxidized and reduced *Clostridium pasteurianum* rubredoxin, J. Am. Chem. Soc. 117 (1995) 5347–5350. https://pubs.acs.org/sharingguidelines.

[39] K.L. Hsueh, W.M. Westler, J.L. Markley, NMR investigations of the rieske protein from thermus thermophilus support a coupled proton and electron transfer mechanism, J. Am. Chem. Soc. 132 (2010) 7908–7918, https://doi.org/10.1021/ja1026387.

[40] C. Caillet-Saguy, M. Delepierre, A. Lecroisey, I. Bertini, M. Piccioli, P. Turano, Direct-detected 13C NMR to investigate the iron(III) hemophore HasA, J. Am. Chem. Soc. 128 (2006) 150–158, https://doi.org/10.1021/ja054902h.

[41] E.C. Cook, G.A. Usher, S.A. Showalter, The use of 13C direct-detect NMR to characterize flexible and disordered proteins, in: Methods in Enzymology, Academic Press Inc., 2018, pp. 81–100, https://doi.org/10.1016/bs.mie.2018.08.025.

[42] M. Kostic, S.S. Pochapsky, T.C. Pochapsky, Rapid recycle 13C′, 15N and 13C, 13C′ heteronuclear and homonuclear multiple quantum coherence detection for resonance assignments in paramagnetic proteins: example of Ni2+−containing acireductone dioxygenase, J. Am. Chem. Soc. 124 (2002) 9054–9055, https://doi.org/10.1021/ja0268480.

[43] I. Bertini, B. Jiménez, M. Piccioli, 13C direct detected experiments: optimization for paramagnetic signals, J. Magn. Reson. 174 (2005) 125–132, https://doi.org/10.1016/j.jmr.2005.01.014.

[44] I.B. Trindade, G. Hernandez, E. Lebègue, F. Barrière, T. Cordeiro, M. Piccioli, R. O. Louro, Conjuring up a ghost: structural and functional characterization of FhuF, a ferric siderophore reductase from E. coli, J. Biol. Inorg. Chem. 26 (2021) 313–326, https://doi.org/10.1007/s00775-021-01854-y.

[45] Iron-Sulfur Proteins Perovskites, Springer Berlin Heidelberg, Berlin, Heidelberg, 1995, https://doi.org/10.1007/3-540-59105-2.

[46] R. Crichton, Biological Inorganic Chemistry: A New Introduction to Molecular Structure and Function, Third edition, Elsevier, 2003.

[47] I. Bertini, H.B. Gray, S.J. Lippard, J.S. Valentine, Bioinorganic chemistry, LibreText (2021). https://LibreTexts.org.

[48] J. Reedijk, Fifty years of inorganic biochemistry: developments, trends, highlights, impact and citations, J. Inorg. Biochem. 212 (2020), https://doi.org/10.1016/j.jinorgbio.2020.111230.

[49] M.C.A. Munn, Researches on myohaematin and the histohaematins, Philos. Trans. R. Soc. Lond. 177 (1886) 267–298, https://doi.org/10.1113/jphysiol.1887.sp000243.

[50] A. Kowalsky, Nuclear magnetic resonance studies of proteins, J. Biol. Chem. 237 (1962) 1807–1819, https://doi.org/237/6/1807.

[51] K. Wüthrich, R.G. Shulman, J. Peisach, High-resolution proton magnetic resonance spectra of sperm whale cyanometmyoglobin, Proc. Natl. Acad. Sci. U. S. A. 60 (1968) 373–380, https://doi.org/10.1073/pnas.60.2.373.

[52] D.C. Blomstrom, E. Knight Jr., W.D. Phillips, J.F. Weiher, The nature of iron in ferredoxin, Proc. Natl Acad. Sci. 51 (1964) 1085–1093, https://doi.org/10.1073/pnas.51.6.1085.

[53] K. Wüthrich, R.G. Shulman, T. Yamane, Proton magnetic resonance studies of human cyanometmyoglobin, Proc. Natl. Acad. Sci. U. S. A. 61 (1968) 1199–1206, https://doi.org/10.1073/pnas.61.4.1199.

[54] M. Poe, W.D. Phillips, C.C. Mcdonald, W. Lovenberg, Proton magnetic resonance study of ferredoxin from *Clostridium pasteurianum**, Proc. Natl. Acad. Sci. 65 (1970) 797–804, https://doi.org/10.1073/pnas.65.4.797.

[55] S.L. Patt, B.D. Sykes, Water eliminated fourier transform NMR spectroscopy, J. Chem. Phys. 56 (1972) 3182–3184, https://doi.org/10.1063/1.1677669.

[56] C.A. Salgueiro, D.L. Turner, H. Santos, J. Legall, A.v. Xavier, Assignment of the redox potentials to the four harms in Desulfovibrio vulgaris cytochrome c3 by 2D-NMR, FEBS J. 314 (1992) 155–158, https://doi.org/10.1016/0014-5793(92)80963-h.

[57] S. Ramaprasad, R.D. Johnson, G.N. La Mar, Vinyl mobility in myoglobin as studied by time- dependent nuclear overhauser effect measurements, J. Am. Chem. Soc. 106 (1984) 3632–3635, https://doi.org/10.1021/ja00324a036.

[58] L. Banci, I. Bertini, L.D. Eltis, I.C. Felli, D.H.W. Kastrau, C. Luchinat, M. Piccioli, R. Pierattelli, M. Smith, The three-dimensional structure in solution of the paramagnetic high-potential iron-sulfur protein I from *Ectothiorhodospira halophila* through nuclear magnetic resonance, Eur. J. Biochem. 225 (1994) 715–725, https://doi.org/10.1111/j.1432-1033.1994.00715.x.

[59] I. Bertini, C. Luchinat, L.-J. Ming, M. Piccioli, M. Sola, J. Selverstone Valentine, Two-dimensional 1H NMR studies of the paramagnetic metalloenzyme copper-nickel superoxide dismutase, Inorg. Chem. 31 (1992) 4433–4435, https://doi.org/10.1021/ic00048a001.

[60] S. Donald Emerson, G.N. la Mar, Solution structural characterization of cyanometmyoglobin: resonance assignment of Heme cavity residues by two-dimensional NMR, Biochemistry. 29 (1990) 1545–1556, https://doi.org/10.1021/bi00458a028.

[61] T.C. Pochapsky, X.M. Ye, G. Ratnaswamy, T.A. Lyons, An NMR-derived model for the solution structure of oxidized Putidaredoxin, a 2-Fe, 2-S ferredoxin from pseudomonas, Biochemistry. 33 (1994) 6424–6432, https://doi.org/10.1021/bi00187a006.

[62] K.L. Bren, H.B. Gray, J. Lucia Banci, I. Bertini, P. Turanos, Paramagnetic lH NMR spectroscopy of the cyanide derivative of Met80Ala-iso-1-cytochrome c, J. Am. Chem. Soc. 117 (1995) 8067–8073, https://doi.org/10.1021/Ja00136A003.

[63] L. Banci, I. Bertini, K.L. Bren, H.B. Gray, P. Sompornpisut, P. Turanot, A.A. Noyes, Three-dimensional solution structure of the cyanide adduct of a Met80Ala variant of *Saccharomyces cerevisiae* Iso-1-cytochrome c. Identification of ligand-residue interactions in the distal heme cavityt, Biochemistry (1995), https://doi.org/10.1021/bi00036a011.

[64] J.-M. Moratal, J. Salgado, A. Donaire, H.R. Jiménez, J. Castells, COSY and NOESY characterization of cobalt(II)-substituted Azurin from *Pseudomonas aeruginosa*, in: Perspectives on Bioinorganic Chemistry 32, 1993, p. 4434, https://doi.org/10.1021/ic00069a006.

[65] A.P. Kalverda, J. Salgado, C. Dennison, G.W. Canters, Analysis of the paramagnetic copper(II) site of amicyanin by 1H NMR spectroscopy, Biochemistry. (1996), https://doi.org/10.1021/bi9518508.

[66] I. Bertini, S. Ciurli, A. Dikiy, C.O. Fernàndez, C. Luchinat, N. Safarov, S. Shumilin, A.J. Vila, The first solution structure of a paramagnetic copper(II) protein: the case of oxidized plastocyanin from the cyanobacterium Synechocystis PCC6803, J. Am. Chem. Soc. 123 (2001) 2405–2413, https://doi.org/10.1021/ja0033685.

[67] H.M. Berman, J. Westbrook, Z. Feng, G. Gilliland, T.N. Bhat, H. Weissig, I. N. Shindyalov, P.E. Bourne, The protein data bank, Nucleic Acids Res. 28 (2000), https://doi.org/10.1093/nar/28.1.235.

[68] R.G. Shulman, S. Ogawa, K. Wuthrich, T. Yamane, J. Peisach, W.E. Blumberg, The absence of "Heme-Heme" interactions in hemoglobin, Science 251 (1969) 1–7, https://doi.org/10.1126/science.165.3890.251.

[69] G.N. la Mar, Isotropic shifts of some ionic complexes of cobalt(II) and nickel(II): evidence for ion pairing, J. Chem. Phys. 41 (1964) 2992–2998, https://doi.org/10.1063/1.1725664.

[70] R.O. Louro, I.J. Correia, L. Brennan, I.B. Coutinho, A.v. Xavier, D.L. Turner, Electronic structure of low-spin ferric porphyrins: 13C NMR studies of the influence of axial ligand orientation, J. Am. Chem. Soc. 120 (1998) 13240–13247, https://doi.org/10.1021/ja983102m.

[71] N. v Shokhirev, F.A. Walker, N. v Shokhirev, F.A. Walker, The effect of axial ligand plane orientation on the contact and pseudocontact shifts of low-spin ferriheme proteins, JBIC. 3 (1998) 581–594, https://doi.org/10.1007/s007750050271.

[72] I. Bertini, C. Luchinat, G. Parigi, Magnetic susceptibility in paramagnetic NMR, Prog. Nucl. Magn. Reson. Spectrosc. 40 (2002) 249–273, https://doi.org/10.1016/j.pnmrs.2019.06.003.

[73] L. Zhong, X. Wen, T.M. Rabinowitz, B.S. Russell, E.F. Karan, K.L. Bren, Heme axial methionine fluxionality in *Hydrogenobacter thermophilus* cytochrome c 552, Proc. Natl. Acad. Sci. 101 (2004) 8637–8642. www.pnas.orgcgidoi10.1073pnas.0402033101.

[74] F.A. Walker, Models of the Bis-histidine-ligated Electron-transferring cytochromes. Comparative Geometric and Electronic Structure of Low-Spin Ferro- and Ferrihemes, Chem. Rev. 104 (2004) 589–615, https://doi.org/10.1021/cr020634j.

[75] R.O. Louro, E.C. de Waal, M. Ubbink, D.L. Turner, Replacement of the methionine axial ligand in cytochrome c550 by a lysine: effects on the haem electronic structure, FEBS Lett. 510 (2002) 185–188, https://doi.org/10.1016/S0014-5793(01)03272-0.

[76] R. Pierattelli, D.L. Turner, L. Banci, R. Pierattelli, L. Banci, D.L. Turner, Indirect determination of magnetic susceptibility tensors in peroxidases: a novel approach to structure elucidation by NMR, JBIC 1 (1996) 320–329, https://doi.org/10.1007/s007750050060.

[77] C. Vicari, I.H. Saraiva, O. Maglio, F. Nastri, V. Pavone, R.O. Louro, A. Lombardi, Artificial heme-proteins: determination of axial ligand orientations through paramagnetic NMR shifts, Chem. Commun. 50 (2014) 3852–3855, https://doi.org/10.1039/c3cc49123d.

[78] O. Maglio, M. Chino, C. Vicari, V. Pavone, R.O. Louro, A. Lombardi, Histidine orientation in artificial peroxidase regioisomers as determined by paramagnetic NMR shifts, Chem. Commun. 57 (2021) 990–993, https://doi.org/10.1039/d0cc06676a.

[79] I. Bertini, C. Luchinat, G. Parigi, F.A. Walker, I. Bertini, C. Luchinat, G. Parigi, F. A. Walker, Heme methyl 1H chemical shifts as structural parameters in some low-spin ferriheme proteins, JBIC 4 (1999) 515–519.

[80] D.L. Turner, Obtaining ligand geometries from paramagnetic shifts in low-spin haem proteins, JBIC 5 (2000) 328–332, https://doi.org/10.1007/pl00010661.

[81] I. Bertini, I.C. Felli, C. Luchinat, High magnetic field consequences on the NMR hyperfine shifts in solution, J. Magn. Reson. (1998), https://doi.org/10.1006/jmre.1998.1507.

[82] L. Banci, I. Bertini, C. Luchinat, R. Pierattelli, N.v. Shokhirev, F.A. Walker, Analysis of the temperature dependence of the 1 H and 13 C isotropic shifts of horse heart Ferricytochrome c: explanation of curie and anti-curie temperature dependence and nonlinear pseudocontact shifts in a common two-level framework, J. Am. Chem. Soc. 120 (1998) 8472–8479.

[83] H. Raanan, D.H. Pike, E.K. Moore, P.G. Falkowski, V. Nanda, Modular origins of biological electron transfer chains, Proc. Natl. Acad. Sci. U. S. A. 115 (2018) 1280–1285, https://doi.org/10.1073/pnas.1714225115.

[84] C. Bonfio, E. Godino, M. Corsini, F. Fabrizi de Biani, G. Guella, S.S. Mansy, Prebiotic iron–sulfur peptide catalysts generate a pH gradient across model membranes of late protocells, Nature Catalysis 1 (2018) 616–623, https://doi.org/10.1038/s41929-018-0116-3.

[85] H. Beinert, R.H. Holm, E. Mü, Iron-sulfur clusters: Nature's modular, multipurpose structures, Science. 277 (1997) 653–659, https://doi.org/10.1126/science.277.5326.653.

[86] L. Banci, I. Bertini, C. Luchinat, The 1H NMR parameters of magnetically coupled dimers - the Fe2S2 proteins as an example, in: Structure and Bonding 72, 1990, pp. 114–136.

[87] L. Skjeldal, J.L. Markley, V.M. Coghlan, L.E. Vickery, 1H NMR spectra of vertebrate [2Fe-2S] ferredoxins. Hyperfine resonances suggest different electron delocalization patterns from plant ferredoxins, Biochemistry. 30 (1991) 9078–9083, https://doi.org/10.1021/bi00101a024.

[88] K. Cai, M. Tonelli, R.O. Frederick, J.L. Markley, Human mitochondrial ferredoxin 1 (FDX1) and ferredoxin 2 (FDX2) both bind cysteine desulfurase and donate electrons for Iron-sulfur cluster biosynthesis, Biochemistry. 56 (2017) 487–499, https://doi.org/10.1021/acs.biochem.6b00447.

[89] B. Xia, D. Jenk, D.M. LeMaster, W.M. Westler, J.L. Markley, Electron-nuclear interactions in two prototypical [2Fe-2S] proteins: selective (chiral) deuteration and analysis of 1H and 2H NMR signals from the alpha and beta hydrogens of cysteinyl residues that ligate the iron in the active sites of human ferredoxin and Anabaena 7120 vegetative ferredoxin, Arch. Biochem. Biophys. 373 (2000) 328–334, https://doi.org/10.1006/abbi.1999.1576.

[90] R.C. Holz, F.J. Small, S.A. Ensign, Proton nuclear magnetic resonance investigation of the proton nuclear magnetic resonance investigation of the [2Fe-2S]1- -containing "Rieske-type" protein from-containing "Rieske-Type" protein from Xanthobacter strain Py2 strain Py2, Biochemistry. 36 (1997) 14690–24696. https://epublications.marquette.edu/chem_fac/303.

[91] P. Bertrand, J.-P. Gayda, J.A. Fee, D. Kuila, R. Cammack, Comparison of the spin-lattice relaxation properties of the two classes of [2Fe-2S] clusters in proteins, Biochim. Biophys. Acta 916 (1987) 24–28, https://doi.org/10.1016/0167-4838(87)90206-8.

[92] G. Toulouse, Theory of the frustation effect in spin glasses: I, Commun. Phys. 2 (1977) 115–119, https://doi.org/10.1142/9789812799371_0009.

[93] O. Kahn, Competing spin interactions and degenerate frustration for discrete molecular species, Chem. Phys. Lett. 265 (1997) 109–114, https://doi.org/10.1016/S0009-2614(96)01424-8.

[94] T.A. Kent, B.H. Huynh, E. Monck, Iron-sulfur proteins: spin-coupling model for three-iron clusters, Proc. Natl. Acad. Sci. 77 (1980) 6574–6576, https://doi.org/10.1073/pnas.77.11.6574.

[95] A.L. Macedo, P. Rodrigues, B.J. Goodfellow, The 3Fe containing ferredoxin from Desulfovibrio gigas: an NMR characterization of the oxidised and intermediate states, Coord. Chem. Rev. (1999) 871–881, https://doi.org/10.1016/s0010-8545(99)00126-5.

[96] A. Dey, T. Glaser, J.J.G. Moura, R.H. Holm, B. Hedman, K.O. Hodgson, E. I. Solomon, Ligand K-edge X-ray absorption spectroscopy and DFT calculations on [Fe3S4]0,+ clusters: delocalization, redox, and effect of the protein environment, J. Am. Chem. Soc. 126 (2004) 16868–16878, https://doi.org/10.1021/ja0466208.

[97] I. Bertini, A. Dikiy, C. Luchinat, R. Macinai, M.S. Viezzoli, M. Vincenzini, An NMR study of the 7Fe-8S ferredoxin from Rhodopseudomonas palustris and reinterpretation of data on similar systems, Biochemistry. 36 (1997) 3570–3579, https://doi.org/10.1021/bi962799q.

[98] V. Papaefthymiou, J. Girerd, I. Moura, J.J.G. Moura, E. Munck, Mossbauer study of *D. gigas* ferredoxin II and spin-coupling model for the Fe3S4 cluster with valence delocalization, J. Am. Chem. Soc. 109 (1987) 6574–6576, https://doi.org/10.1021/ja00249a037.

[99] L. Noodleman, C.Y. Peng, D.A. Case, L.-M. Mouesca, Orbital interactions, electron delocalization and spin coupling in iron-sulfur clusters, Coord. Chem. Rev. 144 (1995) 199–244, https://doi.org/10.1016/0010-8545(95)07011-L.

[100] L. le Pape, B. Lamotte, J.-M. Mouesca, G. Rius, Paramagnetic states of four Iron-four sulfur clusters. 1. EPR single-crystal study of 3+ and 1+ clusters of an asymmetrical model compound and general model for the interpretation of the g-tensors of these two redox states, J. Am. Chem. Soc. 119 (1997) 9757–9770, https://doi.org/10.1021/ja963349o.

[101] I. Bertini, F. Briganti, C. Luchinat, A. Scozzafava, M. Solas, 'H NMR spectroscopy and the electronic structure of the high potential iron-sulfur protein from *Chromatium vinosum*, J. Am. Chem. Soc. 113 (1991) 1237–1245.

[102] L. Banci, I. Bertini, J.S. Ciurli, S. Ferretti, C. Luchinat, M. Picciolit, The electronic structure of [Fe4S4]3+ clusters in proteins. An Investigation of the Oxidized High-Potential Iron-Sulfur Protein II from *Ectothiorhodospira vacuolata*, Biochemistry. 32 (1993) 9387–9397.

[103] A. Bertarello, T. Schubeis, C. Fuccio, E. Ravera, M. Fragai, G. Parigi, L. Emsley, G. Pintacuda, C. Luchinat, Paramagnetic properties of a crystalline Iron-sulfur protein by magic-angle spinning NMR spectroscopy, Inorg. Chem. 56 (2017) 6624–6629, https://doi.org/10.1021/acs.inorgchem.7b00674.

[104] I. Bertini, C. Luchinat, A. Rosato, NMR spectra of Iron-sulfur proteins, Adv. Inorg. Chem. 47 (1999) 251–282, https://doi.org/10.1016/S0898-8838(08)60080-X.

[105] F. Capozzi, C. Luchinat, M. Piccioli, A.J. Vila, I. Bertini, The Fe4S4 centers in ferredoxins studied through proton and carbon hyperfine coupling. Sequence-Specific Assignments of Cysteines in Ferredoxins from Clostridium acidi urici and *Clostridium pasteurianum*, J. Am. Chem. Soc. 116 (1994) 651–660, https://doi.org/10.1021/ja00081a028.

[106] M. Invernici, I.B. Trindade, F. Cantini, R.O. Louro, M. Piccioli, Measuring transverse relaxation in highly paramagnetic systems, J. Biomol. NMR 74 (2020) 431–442, https://doi.org/10.1007/s10858-020-00334-w.

[107] C.C. Page, C.C. Moser, X. Chen, P.L. Dutton, Natural engineering principles of electron tunnelling in biological oxidation±reduction, Nature. 402 (1999) 47–52, https://doi.org/46972.

[108] B.M. Fonseca, C.M. Paquete, C.A. Salgueiro, R.O. Louro, The role of intramolecular interactions in the functional control of multiheme cytochromes c, FEBS Lett. 586 (2012) 504–509, https://doi.org/10.1016/j.febslet.2011.08.019.

[109] M. Ubbink, The courtship of proteins: understanding the encounter complex, FEBS Lett. 583 (2009) 1060–1066, https://doi.org/10.1016/j.febslet.2009.02.046.

[110] I. Ferecatu, S. Gonçalves, M.P. Golinelli-Cohen, M. Clémancey, A. Martelli, S. Riquier, E. Guittet, J.M. Latour, H. Puccio, J.C. Drapier, E. Lescop, C. Bouton, The diabetes drug target MitoNEET governs a novel trafficking pathway to rebuild an Fe-S cluster into cytosolic aconitase/iron regulatory protein 1, J. Biol. Chem. 289 (2014) 28070–28086, https://doi.org/10.1074/jbc.M114.548438.

[111] R. Lill, S.-A. Freibert, Mechanisms of mitochondrial Iron-sulfur protein biogenesis, Annu. Rev. Biochem. 89 (2020) 471–499, https://doi.org/10.1146/annurev-biochem-013118.

[112] N. Maio, B.A.P. Lafont, D. Sil, Y. Li, J.M. Bollinger, C. Krebs, T.C. Pierson, W. M. Linehan, T.A. Rouault, Fe-S cofactors in the SARS-CoV-2 RNA-dependent RNA polymerase are potential antiviral targets, Science. 373 (2021) 236–241, https://doi.org/10.1126/science.abi5224.

[113] D. Suraci, G. Saudino, V. Nasta, S. Ciofi-Baffoni, L. Banci, ISCA1 orchestrates ISCA2 and NFU1 in the maturation of human mitochondrial [4Fe-4S] proteins, J. Mol. Biol. 433 (2021), https://doi.org/10.1016/j.jmb.2021.166924.

[114] D. Brancaccio, A. Gallo, M. Piccioli, E. Novellino, S. Ciofi-Baffoni, L. Banci, [4Fe-4S] cluster assembly in mitochondria and its impairment by copper, J. Am. Chem. Soc. 139 (2017) 719–730, https://doi.org/10.1021/jacs.6b09567.

[115] D. Brancaccio, A. Gallo, M. Mikolajczyk, K. Zovo, P. Palumaa, E. Novellino, M. Piccioli, S. Ciofi-Baffoni, L. Banci, Formation of [4Fe-4S] clusters in the mitochondrial iron-sulfur cluster assembly machinery, J. Am. Chem. Soc. 136 (2014) 16240–16250, https://doi.org/10.1021/ja507822j.

[116] F. Camponeschi, R. Muzzioli, S. Ciofi-Baffoni, M. Piccioli, L. Banci, Paramagnetic 1H NMR spectroscopy to investigate the catalytic mechanism of radical S-adenosylmethionine enzymes, J. Mol. Biol. 431 (2019) 4514–4522, https://doi.org/10.1016/j.jmb.2019.08.018.

[117] R.E. Stenkamp, Dioxygen and hemerythrin, Chem. Rev. 94 (1994) 715–726, https://doi.org/10.1021/cr00027a008.

[118] H. Eklund, U. Uhlin, M. Färnegårdh, D.T. Logan, P. Nordlund, Structure and function of the radical enzyme ribonucleotide reductase, Prog. Biophys. Mol. Biol. 77 (2001) 177–268, https://doi.org/10.1016/s0079-6107(01)00014-1.

[119] W.R. Hagen, P.L. Hagedoorn, K. Honarmand Ebrahimi, The workings of ferritin: a crossroad of opinions, Metallomics. 9 (2017) 595–605, https://doi.org/10.1039/c7mt00124j.

[120] P. Turano, D. Lalli, I.C. Felli, E.C. Theil, I. Bertini, NMR reveals pathway for ferric mineral precursors to the central cavity of ferritin, Proc. Natl. Acad. Sci. U. S. A. 107 (2010) 545–550, https://doi.org/10.1073/pnas.0908082106.

[121] M.J. Maroney, D.M. Kurtz, J.M. Nocek, L.M. Pearce, L. Que, 1H NMR probes of the binuclear iron cluster in hemerythrin, J. Am. Chem. Soc. 108 (1986) 6871–6879, https://doi.org/10.1021/ja00282a005.

[122] J.J.R.F. Silva, R.J.P. Williams, The Biological Chemistry of the Elements, Oxford University Press, 2001.

[123] M.E. Zaballa, L. Ziegler, D.J. Kosman, A.J. Vila, NMR study of the exchange coupling in the trinuclear cluster of the multicopper oxidase Fet3p, J. Am. Chem. Soc. 132 (2010) 11191–11196, https://doi.org/10.1021/ja1037148.

[124] L. Bubacco, J. Salgado, A.W.J.W. Tepper, E. Vijgenboom, G.W. Canters, 1H NMR spectroscopy of the binuclear Cu(II) active site of Streptomyces antibioticus tyrosinase, FEBS Lett. 442 (1999) 215–220, https://doi.org/10.1016/S0014-5793(98)01662-7.

[125] M.C. Machczynski, J.T. Babicz, Correlating the structures and activities of the resting oxidized and native intermediate states of a small laccase by paramagnetic NMR, J. Inorg. Biochem. 159 (2016) 62–69, https://doi.org/10.1016/j.jinorgbio.2016.02.002.

[126] M.A. McGuirl, D.M. Dooley, Copper proteins with type 2 sites, in: Encyclopedia of Inorganic and Bioinorganic Chemistry, John Wiley & Sons, Ltd, 2011, https://doi.org/10.1002/9781119951438.eibc0274.

[127] I. Bertini, R. Pierattelli, Copper(II) proteins are amenable for NMR investigations, pure and applied, Chemistry 76 (2004) 321–333, https://doi.org/10.1351/pac200476020321.

[128] I. Bertini, I.C. Felli, C. Luchinat, G. Parigi, R. Pierattelli, Towards a protocol for solution structure determination of copper(II) proteins: the case of CuIIZnII superoxide dismutase, ChemBioChem. 8 (2007) 1422–1429, https://doi.org/10.1002/cbic.200700006.

[129] J. Salgado, G. Warmerdam, L. Bubacco, G.W. Canters, Understanding the electronic properties of the CuA site from the soluble domain of cytochrome c

oxidase through paramagnetic 1H NMR, Biochemistry. 37 (1998) 7378–7389, https://doi.org/10.1021/bi9728598.
[130] C.O. Fernández, J.A. Cricco, C.E. Slutter, J.H. Richards, H.B. Gray, A.J. Vila, Axial ligand modulation of the electronic structures of binuclear copper sites: analysis of paramagnetic 1H NMR spectra of Met160Gln CuA, J. Am. Chem. Soc. 123 (2001) 11678–11685, https://doi.org/10.1021/ja0162515.
[131] L.A. Abriata, G.N. Ledesma, R. Pierattelli, A.J. Vila, Electronic structure of the ground and excited states of the CuA site by NMR spectroscopy, J. Am. Chem. Soc. 131 (2009) 1939–1945, https://doi.org/10.1021/ja8079669.
[132] N.N. Murthy, K.D. Karlin, I. Bertini, C. Luchinat, NMR and electronic relaxation in paramagnetic Dicopper(II) compounds, J. Am. Chem. Soc. 119 (1997) 2156–2162, https://doi.org/10.1021/ja961555q.
[133] D.F. Hansen, J.J. Led, Determination of the geometric structure of the metal site in a blue copper protein by paramagnetic NMR, Proc. Natl. Acad. Sci. 103 (2006) 1738–1743, https://doi.org/10.1073/pnas.0507179103.
[134] R. Dasgupta, K.B.S.S. Gupta, H.J.M. de Groot, M. Ubbink, Towards resolving the complex paramagnetic nuclear magnetic resonance (NMR) spectrum of small laccase: assignments of resonances to residue-specific nuclei, Magnetic Resonance. 2 (2021) 15–23, https://doi.org/10.5194/mr-2-15-2021.
[135] M.M. Hou, P. Polykretis, E. Luchinat, X. Wang, S.N. Chen, H.H. Zuo, Y. Yang, J. L. Chen, Y. Ye, C. Li, L. Banci, X.C. Su, Solution structure and interaction with copper in vitro and in living cells of the first BIR domain of XIAP, Sci. Rep. 7 (2017), https://doi.org/10.1038/s41598-017-16723-5.
[136] L. Banci, I. Bertini, S. Ciofi-Baffoni, Copper trafficking in biology: an NMR approach, HFSP Journal. 3 (2009) 165–175, https://doi.org/10.2976/1.3078306.
[137] C. Nitsche, G. Otting, Pseudocontact shifts in biomolecular NMR using paramagnetic metal tags, Prog. Nucl. Magn. Reson. Spectrosc. 98 (2017) 20–49, https://doi.org/10.1016/j.pnmrs.2016.11.001.
[138] Q. Miao, W.M. Liu, T. Kock, A. Blok, M. Timmer, M. Overhand, M. Ubbink, A. Double-Armed, Hydrophilic transition metal complex as a paramagnetic NMR probe, Angew. Chem. Int. Ed. 58 (2019) 13093–13100, https://doi.org/10.1002/anie.201906049.
[139] D. Joss, D. Häussinger, Design and applications of lanthanide chelating tags for pseudocontact shift NMR spectroscopy with biomacromolecules, Prog. Nucl. Magn. Reson. Spectrosc. 114–115 (2019) 284–312, https://doi.org/10.1016/j.pnmrs.2019.08.002.
[140] E. Matei, A.M. Gronenborn, 19 F paramagnetic relaxation enhancement: a valuable tool for distance measurements in proteins, Angew. Chem. 128 (2016) 158–162, https://doi.org/10.1002/ange.201508464.
[141] J.A. Tang, J.D. Masuda, T.J. Boyle, R.W. Schurko, Ultra-wideline 27Al NMR investigation of three- and five-coordinate aluminum environments, ChemPhysChem. 7 (2006) 117–130, https://doi.org/10.1002/cphc.200500343.
[142] Y. Liu, Z. Hong, G. Tan, X. Dong, G. Yang, L. Zhao, X. Chen, Z. Zhu, Z. Lou, B. Qian, G. Zhang, Y. Chai, NMR and LC/MS-based global metabolomics to identify serum biomarkers differentiating hepatocellular carcinoma from liver cirrhosis, Int. J. Cancer 135 (2014) 658–668, https://doi.org/10.1002/ijc.28706.
[143] H. Iwahara, Y. Asakura, K. Katahira, M. Tanaka, Prospect of hydrogen technology using proton-conducting ceramics, in: Solid State Ionics, 2004, pp. 299–310, https://doi.org/10.1016/j.ssi.2003.03.001.
[144] J. Wöhnert, K.J. Franz, M. Nitz, B. Imperiali, H. Schwalbe, Protein alignment by a coexpressed lanthanide-binding tag for the measurement of residual dipolar couplings, J. Am. Chem. Soc. 125 (2003) 13338–13339, https://doi.org/10.1021/ja036022d.
[145] I.D. Herath, C. Breen, S.H. Hewitt, T.R. Berki, A.F. Kassir, C. Dodson, M. Judd, S. Jabar, N. Cox, G. Otting, S.J. Butler, A chiral lanthanide tag for stable and rigid attachment to single cysteine residues in proteins for NMR, EPR and time-resolved luminescence studies, Chem. Eur. J. 27 (2021) 13009–13023, https://doi.org/10.1002/chem.202101143.
[146] L.W. Donaldson, N.R. Skrynnikov, W.Y. Choy, D.R. Muhandiram, B. Sarkar, J. D. Forman-Kay, L.E. Kay, Structural characterization of proteins with an attached ATCUN motif by paramagnetic relaxation enhancement NMR spectroscopy, J. Am. Chem. Soc. 123 (2001) 9843–9847, https://doi.org/10.1021/ja011241p.
[147] B. Yu, C.C. Pletka, J. Iwahara, Quantifying and visualizing weak interactions between anions and proteins, Biophys. Computat. Biol. 118 (2021) 1–8, https://doi.org/10.1073/pnas.2015879118/-/DCSupplemental.
[148] A.N. Volkov, J.A.R. Worrall, E. Holtzmann, M. Ubbink, Solution structure and dynamics of the complex between cytochrome c and cytochrome c peroxidase determined by paramagnetic, NMR (2006), https://doi.org/10.1073/pnas.0603551103.
[149] X. Xu, W. Reinle, F. Hannemann, P.v. Konarev, D.I. Svergun, R. Bernhardt, M. Ubbink, Dynamics in a pure encounter complex of two proteins studied by solution scattering and paramagnetic NMR spectroscopy, J. Am. Chem. Soc. 130 (2008) 6395–6403, https://doi.org/10.1021/ja7101357.
[150] C. Tang, J.M. Louis, A. Aniana, J.Y. Suh, G.M. Clore, Visualizing transient events in amino-terminal autoprocessing of HIV-1 protease, Nature. 455 (2008) 693–696, https://doi.org/10.1038/nature07342.
[151] C. Tang, J. Iwahara, G.M. Clore, Visualization of transient encounter complexes in protein-protein association, Nature. 444 (2006) 383–386, https://doi.org/10.1038/nature05201.
[152] R. Hulsker, M.v. Baranova, G.S. Bullerjahn, M. Ubbink, Dynamics in the transient complex of plastocyanin-cytochrome f from Prochlorothrix hollandica, J. Am. Chem. Soc. 130 (2008) 1985–1991, https://doi.org/10.1021/ja077453p.
[153] K.A. Baker, C. Hilty, W. Peti, A. Prince, P.J. Pfaffinger, G. Wider, K. Wiithrich, S. Choe, NMR-derived dynamic aspects of N-type inactivation of a Kv channel suggest a transient interaction with the T1 domain, Biochemistry 45 (2006) 1663–1672, https://doi.org/10.1021/bi0516430.
[154] M. Lee, T. Wang, O.v. Makhlynets, Y. Wu, N.F. Polizzi, H. Wu, P.M. Gosavi, J. Stöhr, I.v. Korendovych, W.F. Degrado, M. Hong, Zinc-binding structure of a catalytic amyloid from solid-state NMR, Proc. Natl. Acad. Sci. U. S. A. 114 (2017) 6191–6196, https://doi.org/10.1073/pnas.1706179114.
[155] G. Marius Clore, J. Iwahara, Theory, practice, and applications of paramagnetic relaxation enhancement for the characterization of transient low-population states of biological macromolecules and their complexes, Chem. Rev. 109 (2009) 4108–4139, https://doi.org/10.1021/cr900033p.
[156] C.A. Softley, M.J. Bostock, G.M. Popowicz, M. Sattler, Paramagnetic NMR in drug discovery, J. Biomol. NMR 74 (2020) 287–309, https://doi.org/10.1007/s10858-020-00322-0.
[157] N.J. Anthis, G.M. Clore, Visualizing transient dark states by NMR spectroscopy, Q. Rev. Biophys. 48 (2015) 35–116, https://doi.org/10.1017/S0033583514000122.
[158] G. Pintacuda, M. John, X.C. Su, G. Otting, NMR structure determination of protein – ligand complexes by lanthanide labeling, Acc. Chem. Res. 40 (2007) 206–212, https://doi.org/10.1021/ar050087z.
[159] L. Banci, I. Bertini, J.G. Huber, C. Luchinat, A. Rosato, Partial orientation of oxidized and reduced cytochrome b5 at high magnetic fields: magnetic susceptibility anisotropy contributions and consequences for protein solution structure determination, J. Am. Chem. Soc. 120 (1998) 12903–12909, https://doi.org/10.1021/ja981791w.
[160] I. Bertini, G. Cavallaro, M. Cosenza, R. Kümmerle, C. Luchinat, M. Piccioli, L. Poggi, Cross correlation rates between curie spin and dipole-dipole relaxation in paramagnetic proteins: the case of cerium substituted Calbindin D9k, J. Biomol. NMR 23 (2002) 115–125, https://doi.org/10.1023/a:1016341507527.
[161] J.C. Hus, D. Marion, M. Blackledge, De novo determination of protein structure by NMR using orientational and long-range order restraints, J. Mol. Biol. 298 (2000) 927–936, https://doi.org/10.1006/jmbi.2000.3714.
[162] C.D. Schwieters, J.J. Kuszewski, N. Tjandra, G.M. Clore, The Xplor-NIH NMR molecular structure determination package, Journal of Magnetic Resonance 160 (2003) 65–73, https://doi.org/10.1016/S1090-7807(02)00014-9.
[163] T. Herrmann, P. Güntert, K. Wüthrich, Protein NMR structure determination with automated NOE-identification in the NOESY spectra using the new software ATNOS, J. Biomol. NMR (2002), https://doi.org/10.3929/ethz-b-000422784.
[164] L. Banci, I. Bertini, G. Cavallaro, A. Giachetti, C. Luchinat, G. Parigi, Paramagnetism-based restraints for Xplor-NIH, J. Biomol. NMR 28 (2004) 249–261, https://doi.org/10.1023/B:JNMR.0000013703.30623.f7.
[165] P. Güntert, Automated NMR structure calculation with CYANA, in: Methos in Molecular Biology, 2004, pp. 353–378, https://doi.org/10.1385/1–59259–809-9:353.
[166] J. Iwahara, C.D. Schwieters, G.M. Clore, Ensemble approach for NMR structure refinement against 1H paramagnetic relaxation enhancement data arising from a flexible paramagnetic group attached to a macromolecule, J. Am. Chem. Soc. 126 (2004) 5879–5896, https://doi.org/10.1021/ja031580d.
[167] E.M. Yilmaz, P. Güntert, NMR structure calculation for all small molecule ligands and non-standard residues from the PDB chemical component dictionary, J. Biomol. NMR 63 (2015) 21–37, https://doi.org/10.1007/s10858-015-9959-y.
[168] L. Banci, I. Bertini, K.L. Bren, H.B. Gray, P. Sompornpisut, P. Turanot, A.A. Noyes, Three-dimensional solution structure of the cyanide adduct of a Met80Ala variant of *Saccharomyces cerevisiae* Iso-1-cytochrome c. Identification of ligand-residue interactions in the distal heme cavity, Biochemistry 34 (1995) 11385–11398, https://doi.org/10.1021/bi00036a011.
[169] A.C. Messias, D.H.W. Kastrau, H.S. Costa, J. Legall, D.L. Turner, H. Santos, A.Â. Nio, V. Xavier, Solution structure of *Desulfovibrio vulgaris* (Hildenborough) ferrocytochrome c3: structural basis for functional cooperativity, J. Mol. Biol. 281 (1998) 719–739, https://doi.org/10.1006/jmbi.1998.1974.
[170] O. Karmi, H.B. Marjault, L. Pesce, P. Carloni, J.N. Onuchic, P.A. Jennings, R. Mittler, R. Nechushtai, The unique fold and lability of the [2Fe-2S] clusters of NEET proteins mediate their key functions in health and disease, J. Biol. Inorg. Chem. 23 (2018) 599–612, https://doi.org/10.1007/s00775-018-1538-8.
[171] A.T.P. Carvalho, M. Swart, Electronic structure investigation and parametrization of biologically relevant iron-sulfur clusters, J. Chem. Inf. Model. 54 (2014) 613–620, https://doi.org/10.1021/ci400718m.
[172] F. Autenrieth, E. Tajkhorshid, J. Baudry, Z. Luthey-Schulten, Classical force field parameters for the heme prosthetic group of cytochrome c, J. Comput. Chem. 25 (2004) 1613–1622, https://doi.org/10.1002/jcc.20079.
[173] D. Sakakibara, A. Sasaki, T. Ikeya, J. Hamatsu, T. Hanashima, M. Mishima, M. Yoshimasu, N. Hayashi, T. Mikawa, M. Wälchli, B.O. Smith, M. Shirakawa, P. Güntert, Y. Ito, Protein structure determination in living cells by in-cell NMR spectroscopy, Nature. 458 (2009) 102–105, https://doi.org/10.1038/nature07814.
[174] B. Bin Pan, F. Yang, Y. Ye, Q. Wu, C. Li, T. Huber, X.C. Su, 3D structure determination of a protein in living cells using paramagnetic NMR spectroscopy, Chem. Commun. 52 (2016) 10237–10240, https://doi.org/10.1039/c6cc05490k.
[175] M. Atanasov, D. Aravena, E. Suturina, E. Bill, D. Maganas, F. Neese, First principles approach to the electronic structure, magnetic anisotropy and spin relaxation in mononuclear 3d-transition metal single molecule magnets, Coord. Chem. Rev. 289–290 (2015) 177–214, https://doi.org/10.1016/j.ccr.2014.10.015.
[176] E. Ravera, L. Gigli, B. Czarniecki, L. Lang, R. Kümmerle, G. Parigi, M. Piccioli, F. Neese, C. Luchinat, A quantum chemistry view on two archetypical paramagnetic pentacoordinate nickel(II) complexes offers a fresh look on their NMR spectra, Inorg. Chem. 60 (2021) 2068–2075, https://doi.org/10.1021/acs.inorgchem.0c03635.

[177] L. Lang, E. Ravera, G. Parigi, C. Luchinat, F. Neese, Solution of a puzzle: high-level quantum-chemical treatment of pseudocontact chemical shifts confirms classic semiempirical theory, J. Phys. Chem. Lett. 11 (2020) 8735–8744, https://doi.org/10.1021/acs.jpclett.0c02462.

[178] P. John Cherry, S. Awais Rouf, J. Vaara, Paramagnetic enhancement of nuclear spin-spin coupling, J. Chem. Theory Comput. 13 (2017) 1275–1283, https://doi.org/10.1021/acs.jctc.6b01080.

[179] E.A. Suturina, I. Kuprov, Pseudocontact shifts from mobile spin labels, Phys. Chem. Chem. Phys. 18 (2016) 26412–26422, https://doi.org/10.1039/c6cp05437d.

[180] L. Benda, J. Mareš, E. Ravera, G. Parigi, C. Luchinat, M. Kaupp, J. Vaara, Pseudocontact NMR shifts over the paramagnetic metalloprotein CoMMP-12 from first principles, Angew. Chem. 128 (2016) 14933–14937, https://doi.org/10.1002/ange.201608829.

[182] H.W. Orton, G. Otting, Accurate electron-nucleus distances from paramagnetic relaxation enhancements, J. Am. Chem. Soc. 140 (2018) 7688–7697, https://doi.org/10.1021/jacs.8b03858.

[183] G. Pintacuda, A. Kaikkonen, G. Otting, Modulation of the distance dependence of paramagnetic relaxation enhancements by CSA×DSA cross-correlation, J. Magn. Reson. 171 (2004) 233–243, https://doi.org/10.1016/j.jmr.2004.08.019.

[184] G. Pintacuda, A. Moshref, A. Leonchiks, A. Sharipo, & Gottfried Otting, site-specific labelling with a metal chelator for protein-structure refinement, J. Biomol. NMR 29 (2004) 351–361, https://doi.org/10.1023/B:JNMR.0000032610.17058.fe.

[185] W.R. Hagen, Very low-frequency broadband electron paramagnetic resonance spectroscopy of metalloproteins, J. Phys. Chem. A 125 (2021) 3208–3218, https://doi.org/10.1021/acs.jpca.1c01217.

[186] I. Trindade, M. Invernici, F. Cantini, R. Louro, M. Piccioli, NOE-Less Protein Structures-an Alternative Paradigm in Highly Paramagnetic Systems, FEBS J 288 (2021) 3010–3023.

[187] N.M. Good, R.S. Moore, C.J. Suriano, N.C. Martinez-Gomez, Contrasting in vitro and in vivo methanol oxidation activities of lanthanide-dependent alcohol dehydrogenases XoxF1 and ExaF from *Methylobacterium extorquens* AM1, Sci. Rep. 9 (2019), https://doi.org/10.1038/s41598-019-41043-1.

[188] E.C. Cook, E.R. Featherston, S.A. Showalter, J.A. Cotruvo, Structural basis for rare earth element recognition by *Methylobacterium extorquens* lanmodulin, Biochemistry. 58 (2019) 120–125, https://doi.org/10.1021/acs.biochem.8b01019.